Article

APRIL limits atherosclerosis by binding to heparan sulfate proteoglycans

https://doi.org/10.1038/s41586-021-03818-3

Received: 14 June 2019

Accepted: 12 July 2021

Published online: 25 August 2021

Check for updates

Dimitrios Tsiantoulas[1]✉, Mahya Eslami[2], Georg Obermayer[1,3], Marc Clement[4], Diede Smeets[1], Florian J. Mayer[1], Máté G. Kiss[1,3], Lennart Enders[3], Juliane Weißer[3], Laura Göderle[1,3], Jordi Lambert[4], Florian Frommlet[5], André Mueller[3], Tim Hendrikx[1], Maria Ozsvar-Kozma[1,3], Florentina Porsch[1,3], Laure Willen[2], Taras Afonyushkin[1,3], Jane E. Murphy[4], Per Fogelstrand[6], Olivier Donzé[7], Gerard Pasterkamp[8], Matthias Hoke[9], Stefan Kubicek[3], Helle F. Jørgensen[4], Nicolas Danchin[10,11], Tabassome Simon[12,13], Hubert Scharnagl[14], Winfried März[14,15,16], Jan Borén[6], Henry Hess[17], Ziad Mallat[4,18,19], Pascal Schneider[2,19] & Christoph J. Binder[1,3]✉

Atherosclerotic cardiovascular disease causes heart attacks and strokes, which are the leading causes of mortality worldwide[1]. The formation of atherosclerotic plaques is initiated when low-density lipoproteins bind to heparan-sulfate proteoglycans (HSPGs)[2] and become trapped in the subendothelial space of large and medium size arteries, which leads to chronic inflammation and remodelling of the artery wall[2]. A proliferation-inducing ligand (APRIL) is a cytokine that binds to HSPGs[3], but the physiology of this interaction is largely unknown. Here we show that genetic ablation or antibody-mediated depletion of APRIL aggravates atherosclerosis in mice. Mechanistically, we demonstrate that APRIL confers atheroprotection by binding to heparan sulfate chains of heparan-sulfate proteoglycan 2 (HSPG2), which limits the retention of low-density lipoproteins, accumulation of macrophages and formation of necrotic cores. Indeed, antibody-mediated depletion of APRIL in mice expressing heparan sulfate-deficient HSPG2 had no effect on the development of atherosclerosis. Treatment with a specific anti-APRIL antibody that promotes the binding of APRIL to HSPGs reduced experimental atherosclerosis. Furthermore, the serum levels of a form of human APRIL protein that binds to HSPGs, which we termed non-canonical APRIL (nc-APRIL), are associated independently of traditional risk factors with long-term cardiovascular mortality in patients with atherosclerosis. Our data reveal properties of APRIL that have broad pathophysiological implications for vascular homeostasis.

APRIL is encoded by the tumour necrosis factor ligand superfamily member 13 gene (*Tnfsf13*) and is produced by myeloid cells and stromal cells[4]. APRIL is involved in antibody class switching[5] and plasma cell survival[6,7] in mice and humans through its binding to two receptors—TACI (transmembrane activator and CAML interactor) and BCMA (B cell maturation antigen), respectively—with the same binding site[8]. Patients with coronary artery disease have increased APRIL levels in plasma compared to sex- and age-matched healthy individuals[9], but its role in atherosclerosis remains unclear.

Low-density lipoprotein (LDL) receptor-deficient mice lacking APRIL (*Ldlr*$^{-/-}$*Tnfsf13*$^{-/-}$ mice) that were fed with an atherogenic diet developed larger plaques (Fig. 1a) in the aortic root than their littermate controls, despite having similar cholesterol and triglyceride levels in plasma (Fig. 1d, Extended Data Fig. 1a). Aortic root plaques from *Ldlr*$^{-/-}$*Tnfsf13*$^{-/-}$ mice had enhanced necrotic core and acellular areas (Fig. 1b, Extended Data Fig. 1b) and larger macrophage content (Fig. 1c). The smooth muscle cell content (Extended Data Fig. 1c) and collagen deposition (Extended Data Fig. 1d) in plaques in the aortic root, and plaque size in the thoraco-abdominal aorta, were not affected (Extended Data Fig. 1a). APRIL deficiency did not alter the numbers of splenic B cell (Fig. 1e), splenic T cell (Extended Data Fig. 1e) or peritoneal B cell subsets (Extended Data Fig. 1f), or circulating monocytes (Extended Data Fig. 1g). Besides total IgA, which was moderately reduced in APRIL-deficient mice, total immunoglobulin levels in plasma were

[1]Department of Laboratory Medicine, Medical University of Vienna, Vienna, Austria. [2]Department of Biochemistry, University of Lausanne, Epalinges, Switzerland. [3]CeMM Research Center for Molecular Medicine of the Austrian Academy of Sciences, Vienna, Austria. [4]Division of Cardiovascular Medicine, Department of Medicine, University of Cambridge, Cambridge, UK. [5]Center for Medical Statistics, Informatics and Intelligent Systems, Medical University of Vienna, Vienna, Austria. [6]Institute of Medicine, University of Gothenburg, Göteborg, Sweden. [7]Adipogen Life Sciences, Epalinges, Switzerland. [8]University Medical Center Utrecht, Utrecht, the Netherlands. [9]Department of Internal Medicine II, Medical University of Vienna, Vienna, Austria. [10]Assistance Publique-Hôpitaux de Paris (AP-HP), Hôpital Européen Georges Pompidou, Department of Cardiology, Paris, France. [11]University School of Medicine, Université de Paris, Paris, France. [12]Assistance Publique-Hôpitaux de Paris (AP-HP), Hôpital Saint Antoine, Department of Clinical Pharmacology and Clinical Research Platform of East of Paris (URCEST-CRB-CRC), Paris, France. [13]Department of Pharmacology, Sorbonne-Université (UPMC-Paris 06), Paris, France. [14]Clinical Institute of Medical and Chemical Laboratory Diagnostics, Medical University of Graz, Graz, Austria. [15]Medical Clinic V, Medical Faculty Mannheim, University of Heidelberg, Mannheim, Germany. [16]SYNLAB Academy, Synlab Holding Deutschland GmbH, Augsburg, Germany. [17]Translational Innovation Platform Immunology, Merck KGaA, Darmstadt, Germany. [18]Université de Paris and INSERM U970, Paris Cardiovascular Research Center, Paris, France. [19]These authors contributed equally: Ziad Mallat, Pascal Schneider. ✉e-mail: dimitris.tsiantoulas@meduniwien.ac.at; christoph.binder@meduniwien.ac.at

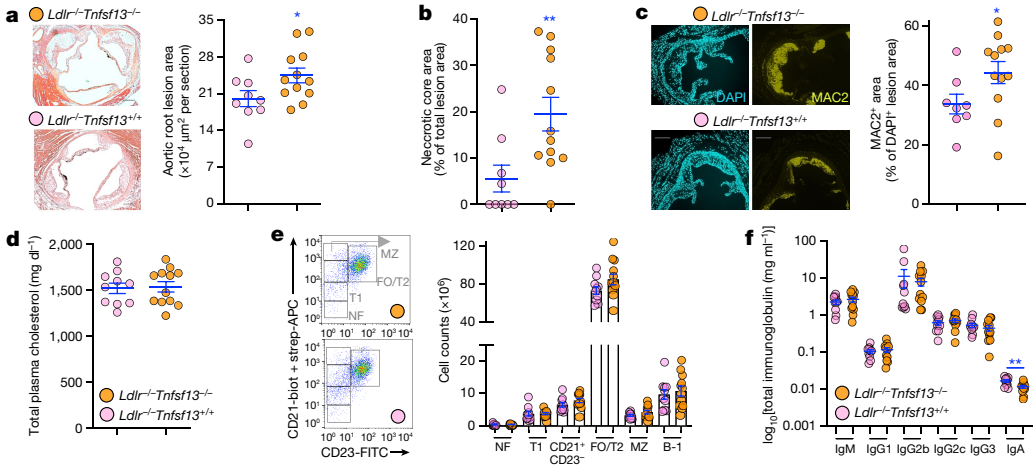

Fig. 1 | APRIL deficiency promotes atherosclerosis. a, Representative photomicrographs of haematoxylin and eosin (H&E)-stained lesions in the aortic origin (left) and lesion size (right; $n = 9$ *Ldlr*$^{-/-}$*Tnfsf13*$^{+/+}$ mice, $n = 12$ *Ldlr*$^{-/-}$*Tnfsf13*$^{-/-}$ mice; $P = 0.041$). **b**, Necrotic core size ($n = 9$ *Ldlr*$^{-/-}$*Tnfsf13*$^{+/+}$ mice, $n = 12$ *Ldlr*$^{-/-}$*Tnfsf13*$^{-/-}$ mice; $P = 0.009$). **c**, Representative photomicrographs (left) and quantification (right) of the MAC2$^+$ area in aortic root lesions (staining for macrophages; $n = 8$ *Ldlr*$^{-/-}$*Tnfsf13*$^{+/+}$ mice, $n = 12$ *Ldlr*$^{-/-}$*Tnfsf13*$^{-/-}$ mice; $P = 0.047$). **d**, Total plasma cholesterol ($n = 10$ *Ldlr*$^{-/-}$*Tnfsf13*$^{+/+}$ mice, $n = 12$ *Ldlr*$^{-/-}$*Tnfsf13*$^{-/-}$ mice). **e**, Flow cytometry plots (left) and absolute numbers (right) of splenic follicular/transitional stage 2 (FO/T2), marginal zone (MZ) CD21$^+$CD23$^-$, transitional stage 1 (T1), newly formed (NF) and B-1 B cells ($n = 10$ *Ldlr*$^{-/-}$*Tnfsf13*$^{+/+}$ mice, $n = 12$ *Ldlr*$^{-/-}$*Tnfsf13*$^{-/-}$ mice). **f**, Total plasma antibody titres ($n = 10$ *Ldlr*$^{-/-}$*Tnfsf13*$^{+/+}$ mice, $n = 12$ *Ldlr*$^{-/-}$*Tnfsf13*$^{-/-}$ mice). All results shown as mean ± s.e.m. $^*P < 0.05$, $^{**}P < 0.01$, (two-tailed Mann–Whitney *U*-test or two-tailed unpaired Student *t*-test). Scale bars, 200 µm.

similar between the groups (Fig. 1f). APRIL binds with high affinity to BCMA[4]. *Ldlr*$^{-/-}$ mice lacking BCMA in the haematopoietic system (*Ldlr*$^{-/-}$*hem-Bcma*$^{-/-}$ mice; Extended Data Fig. 2a) had similar atherosclerosis to *Ldlr*$^{-/-}$*hem-Bcma*$^{+/+}$ controls (Extended Data Fig. 2b, c). Triglyceride (Extended Data Fig. 2c) and total cholesterol levels (Extended Data Fig. 2d) in plasma did not differ between the groups. In contrast to APRIL-deficient mice, *Ldlr*$^{-/-}$*hem-Bcma*$^{-/-}$ mice displayed altered B cell numbers and plasma immunoglobulin levels compared to *Ldlr*$^{-/-}$*hem-Bcma*$^{+/+}$ controls (Extended Data Fig. 2e–h). These data suggest that APRIL confers an atheroprotective effect that is independent of B cell immunity.

Tnfsf13 gene expression levels are high in healthy human arteries (Extended Data Fig. 3a). We show that *Tnfsf13* transcripts are present at intermediate to high levels within the total transcriptome of isolated primary vascular smooth muscle cells from the aortas of healthy mice (Extended Data Fig. 3b, c). Similarly, human umbilical artery smooth muscle cells express *Tnfsf13* (Extended Data Fig. 3d). Moreover, we found that in human atherosclerotic plaques, APRIL comprises approximately 0.5% of the total plaque protein content (Fig. 2a). APRIL, which was present in both human carotid and coronary arteries (Fig. 2b), was enriched at the basement membrane of the endothelial cell layer as well as on the surface of endothelial cells in both atherosclerotic and non-atherosclerotic specimens (Fig. 2c, d). Furthermore, both recombinant mouse and human multimeric flag-tagged APRIL protein (Flag–APRIL) bound to human umbilical vein endothelial cells (HUVECs), and this binding was blocked in the presence of heparin (Extended Data Fig. 4a, b), which shows that APRIL binds to the endothelium via its heparan sulfate binding site[3]. Therefore, we conducted an anti-Flag pull-down assay using HUVECs treated with Flag–APRIL or Flag–control constructs followed by mass spectrometry, and determined that HSPG2 interacts with APRIL (Extended Data Fig. 4c). HSPG2 is an essential component of basement membranes[10] and has been shown to promote the formation of atherosclerotic plaques[11]. The interaction of APRIL and HSPG2 was validated by enzyme-linked immunosorbent assays (ELISAs) using HSPG preparations isolated from mouse basement membranes (Extended Data Fig. 4d). Furthermore, APRIL co-localized with HSPG2 in the subendothelial basement membrane of human arteries with (Pearson's coefficient $r = 0.785$) or without atherosclerosis ($r = 0.687$) (Fig. 2e). In addition, mouse multimeric Flag–APRIL exogenously added to cryosections of mouse arteries (Extended Data Fig. 4e) bound preferentially to arterial areas enriched in HSPG2, and this interaction was meditated exclusively by APRIL's HSPG-binding site, as it was inhibited by heparin (Extended Data Fig. 4f). Furthermore, a surface plasmon resonance analysis showed that both total human (dissociation constant (K_D) = 0.24×10^{-6} M) and mouse APRIL ($K_D = 1.6 \times 10^{-6}$ M) specifically bind to heparan sulfate (Extended Data Fig. 4g).

To investigate whether APRIL mediates its atheroprotective effects by binding to HSPG2, we treated apolipoprotein E-deficient mice, which express HSPG2 lacking heparan sulfate chains (*Apoe*$^{-/-}$*Hspg2*$^{\Delta 3}$), and control mice with either a depleting mouse anti-mouse APRIL antibody (clone 108; Extended Data Fig. 5a–c) or an isotype antibody for seven weeks, and fed the mice with an atherogenic diet for the last six weeks of antibody treatment. In agreement with the proatherogenic role of APRIL deficiency (Fig. 1), antibody-mediated depletion of APRIL increased atherosclerosis in *Apoe*$^{-/-}$*Hspg2*^{wt} mice, but had no effect in *Apoe*$^{-/-}$*Hspg2*$^{\Delta 3}$ mice (Fig. 2f, g). Plasma cholesterol levels were similar among all experimental groups (Fig. 2h).

The heparan sulfate chains of HSPG2 facilitate the retention of LDL in the subendothelial space[11]. Pre-treatment of sections of a mouse carotid artery with APRIL decreased arterial retention of native human LDL (Extended Data Fig. 6a). We obtained similar data using HEK293 wild-type cells (which carry HSPGs), which were incubated with human LDL in the presence of recombinant human APRIL (Extended Data Fig. 6b). In vivo, *Ldlr*$^{-/-}$*Tnfsf13*$^{-/-}$ mice (Fig. 1) show increased apolipoprotein B (ApoB) content in their atherosclerotic plaques compared to controls (Extended Data Fig. 6c). Together, these data show that the HSPG-binding site of APRIL exerts atheroprotective effects by limiting LDL retention in the subendothelial space. However, HSPGs are also involved in other biological processes that have been implicated in atherogenesis, such as monocyte adhesion[12,13]. We found that atherosclerotic lesions in *Ldlr*$^{-/-}$*Tnfsf13*$^{-/-}$ mice have increased macrophage content (Fig. 1c), which could be mediated through a direct effect of the APRIL–HSPG interaction on immune cell recruitment. Consistent with our findings that the protective effect of APRIL is exerted locally in the artery wall, overexpression of human APRIL in T cells does not alter plaque size in *Apoe*$^{-/-}$ mice[14].

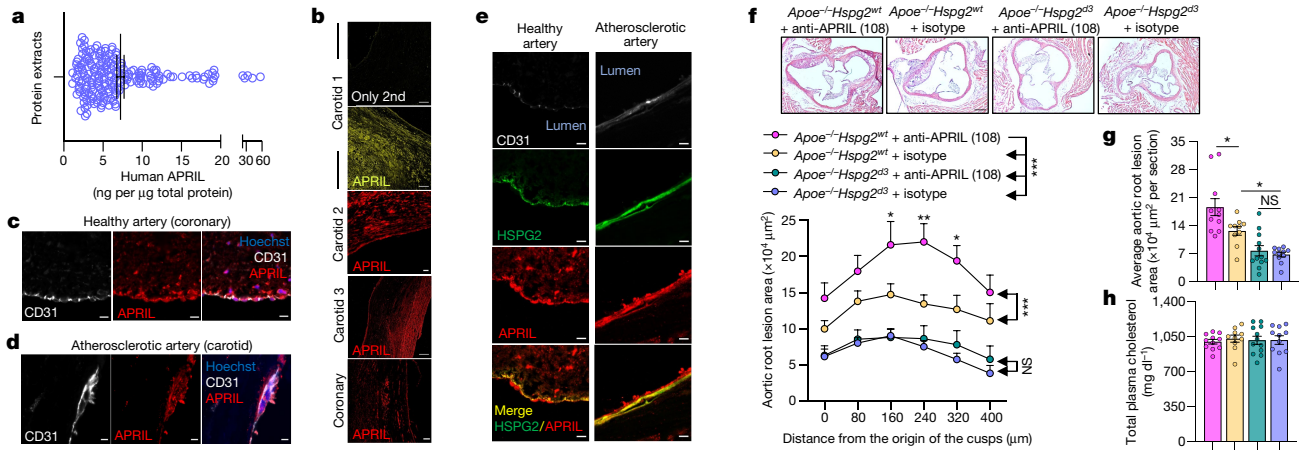

Fig. 2 | APRIL protects against atherosclerosis by binding to HSPG2. **a**, Amount of APRIL in denatured protein lysates of human atherosclerotic plaque extracts ($n = 199$ samples). **b**–**e**, Immunofluorescence analysis of human carotid and coronary artery specimens stained with an anti-APRIL antibody (**b**) (or secondary antibody only; 2nd only), and human coronary and carotid artery specimens with or without atherosclerosis stained with anti-APRIL and anti-CD31 antibodies (**c**, **d**) and stained with anti-APRIL, anti-CD31 and anti-HSPG2 antibodies (**e**). **f**, Representative photomicrographs of H&E-stained lesions (top) and total lesion area in the aortic origin (bottom; 160 µm, $P = 0.037$; 240 µm, $P = 0.004$; 320 µm, $P = 0.045$). **g**, Average lesion size in the aortic origin expressed as µm² per section (*Apoe*$^{-/-}$*Hspg2*^{wt} treated with 108 versus *Apoe*$^{-/-}$*Hspg2*^{wt} treated with isotype, $P = 0.026$; *Apoe*$^{-/-}$*Hspg2*^{wt} treated with isotype versus *Apoe*$^{-/-}$*Hspg2*^{d3} treated with isotype, $P = 0.028$). **h**, Total plasma cholesterol. **f**–**h**, Results shown as mean ± s.e.m. of $n = 11$ *Apoe*$^{-/-}$*Hspg2*^{wt} mice treated with 108; $n = 10$ *Apoe*$^{-/-}$*Hspg2*^{wt} mice treated with isotype; $n = 12$ *Apoe*$^{-/-}$*Hspg2*^{d3} mice treated with 108; $n = 11$ *Apoe*$^{-/-}$*Hspg2*^{d3} mice treated with isotype. $^*P < 0.05$, $^{**}P < 0.01$, $^{***}P < 0.001$ (one-way ANOVA and Tukey's test, two-way ANOVA and Sidak's test). Scale bars: **b**, carotid 1 and 3, 100 µm, carotid 2, 20 µm and coronary, 50 µm; **c**, 10 µm; **d**, 5 µm; **e**, 10 µm; **f**, 200 µm.

We hypothesized that an intervention that promotes binding of APRIL to HSPGs would be beneficial in atherosclerosis. First, we tested a mouse TACI-Ig (a decoy TACI receptor that blocks the TACI/BCMA binding site of APRIL[15]). Treatment with TACI-Ig did not alter atherosclerosis in *Apoe*$^{-/-}$ mice fed an atherogenic diet (Fig. 3a, b). However, TACI-Ig also targets BAFF, which has an atheroprotective role in experimental atherosclerosis[16]. Consistent with its BAFF-depleting activities[16], treatment with TACI-Ig led to depletion of B cells (Extended Data Fig. 7a–e) and a reduction in atheroprotective IgM antibodies[17] in plasma (Extended Data Fig. 7f). To target APRIL alone, we treated *Apoe*$^{-/-}$ mice with an anti-mouse APRIL antibody (clone Apry-1-1; Extended Data Fig. 5a–c) that has selective specificity for the BCMA/TACI-binding site of APRIL[15] and simultaneously increases binding to HSPGs (Fig. 3c) without affecting the stability or levels of APRIL in plasma in vivo (Extended Data Fig. 7g). Treatment with this antibody reduced atherosclerosis in both the aortic root and thoraco-abdominal aorta of *Apoe*$^{-/-}$ mice (Fig. 3a, b), while it preserved B cells and plasma IgM antibodies (Extended Data Fig. 7a–f) and did not affect plasma cholesterol and triglyceride levels or body weight (Extended Data Fig. 7h).

By validating different ELISA systems for the detection of human APRIL, we found that human serum contains an additional and previously unknown (to our knowledge) form of APRIL, hereafter termed non-canonical (nc-)APRIL. This was evidenced when APRIL was depleted from sera or from an APRIL standard either with TACI-Ig or with an anti-APRIL antibody (Aprily2) that recognizes APRIL by immunohistochemistry and western blot (Figs. 2b–e, 4b). Only TACI-Ig, but not Aprily2, could deplete the signal in an APRIL ELISA (ELISA 1). Conversely, only the Aprily2 antibody, but not TACI-Ig, could deplete the signal in another APRIL-specific ELISA (ELISA 2; Fig. 4a–c). We confirmed these data by additional depletion experiments using different anti-human APRIL antibodies (Extended Data Fig. 8a–g). APRIL detected in serum by ELISA 2 could be depleted by several monoclonal antibodies (Aprily1, 2, 5, 6, 8) that recognize at least two different epitopes, without affecting the detection of the canonical form of APRIL (c-APRIL)

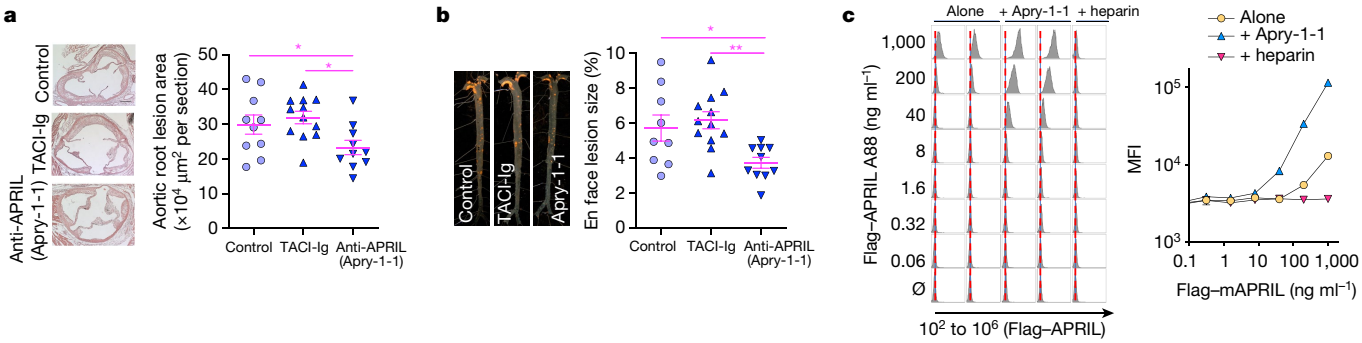

Fig. 3 | Antibody targeting of APRIL at the BCMA/TACI binding site reduces atherosclerosis. *Apoe*$^{-/-}$ mice were treated with a mixture of anti-mouse APRIL antibody (Apry-1-1) and control Ig (anti-APRIL group), or TACI-Ig and isotype IgG2b (TACI-Ig group), or isotype IgG2b and control Ig (control group). **a**, Representative photomicrographs of H&E-stained lesions (left) and lesion size in the aortic origin (right; $n = 10$ control, $n = 12$ TACI-Ig, $n = 10$ anti-APRIL; $P = 0.025$). Scale bar, 200 µm. **b**, Representative photomicrographs of Sudan-IV stained aortas (left) and en face lesion size (right; $n = 9$ control, $n = 12$ TACI-Ig, $n = 10$ anti-APRIL; $P = 0.006$). **c**, HEK293 wild-type cells were stained with Flag–ACRP–mAPRIL A88 (multimeric APRIL) that was preincubated or not with anti-APRIL antibody Apry-1-1 or heparin and analysed by flow cytometry. MFI, mean fluorescence intensity. Data are representative of two independent experiments performed in duplicate. All results show mean ± s.e.m. (**c**, error bars are smaller than symbols). $^*P < 0.05$, $^{**}P < 0.01$ (one-way ANOVA and Newman–Keuls test).

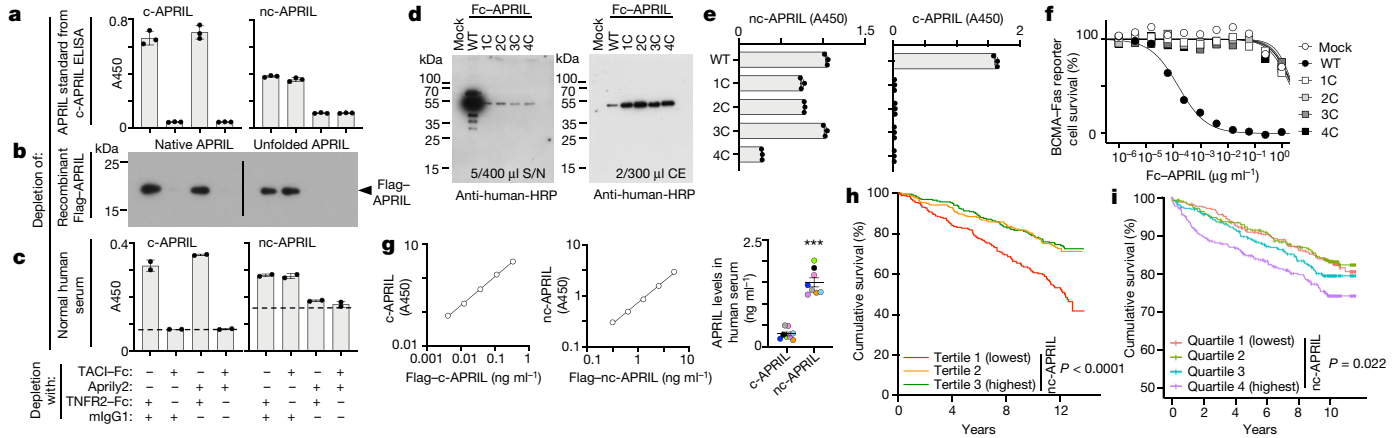

Fig. 4 | Circulating nc-APRIL levels predict cardiovascular mortality in humans. a, APRIL standard of c-APRIL-specific ELISA was depleted twice with beads coupled to a recombinant APRIL receptor (TACI-Ig) or to a control receptor (TNFR2-Ig), or with beads coupled to an anti-APRIL monoclonal antibody (Aprily2) or to an isotype-matched control (mIgG1), in the indicated combinations (bottom of **c**). Unbound fractions were measured for APRIL using nc-APRIL-specific (right) or c-APRIL-specific ELISA (left). **b**, Recombinant Flag–APRIL in native or unfolded states was depleted once with the indicated bead combinations. Unbound fractions were analysed by anti-Flag western blot. **c**, Human serum from a healthy individual was depleted twice with the indicated combinations of beads, then analysed for APRIL content with nc-APRIL-specific (right) or c-APRIL-specific ELISA (left). **d**, Fc–human APRIL (wild-type, WT; amino acids 98–233) and Fc-APRIL with C-terminal truncations of 1, 2, 3, or 4 amino acids (1C–4C) were transfected into HEK-293T cells, and supernatants (S/N) and cell extracts (CE) were analysed by reducing western blot. **e**, Fc–APRIL with or without C-terminal truncations was measured with c-APRIL-specific (left) or nc-APRIL-specific ELISA (right). **f**, Supernatants adjusted for APRIL concentrations were tested for activity on BCMA–Fas reporter cells. **g**, Quantified c-APRIL was used as a standard in the c-APRIL-specific ELISA (left) and quantified purified nc-APRIL was used as a standard in the nc-APRIL-specific ELISA (middle). Using these standard curves, the concentrations of c-APRIL and nc-APRIL were measured by ELISA in sera from healthy individuals (right; $n = 8$, two-tailed paired Student's t-test, $^{***}P < 0.001$). **h**, **i**, Serum levels of nc-APRIL were associated with cardiovascular mortality in asymptomatic individuals from ICARAS (**h**) and in symptomatic patients from LURIC (**i**). Data are representative of three (**a**–**c**, **e**) and two (**d**, **g**) independent experiments. **a**, **c**, **e**, **g**, Results show mean ± s.e.m. **h**, **i**, See Methods for description of statistical analysis.

by ELISA 1 (Extended Data Fig. 8h, i). Moreover, depletion of human APRIL in serum by antibodies (clones Mahya1 and 110.6) or biologicals (Atacicept; human TACI-Fc fusion protein) that are directed against c-APRIL did not affect the detection of nc-APRIL by ELISA 2 (Extended Data Fig. 8i). Thus, both ELISAs are specific but recognize different forms of APRIL. ELISA 2 recognizes nc-APRIL, which cannot bind the immune receptor TACI. However, both nc-APRIL and c-APRIL bind to heparan sulfates with equivalent affinities ($K_D = 6.3 \times 10^{-7}$ M and $K_D = 2.6 \times 10^{-7}$ M, respectively; Extended Data Fig. 4g). Flag-tagged c-APRIL and nc-APRIL showed markedly different sizes upon gel filtration under native conditions. c-APRIL eluted as a trimer and nc-APRIL as a much larger multimer (Extended Data Fig. 8j–n). Furthermore, nc-APRIL and c-APRIL are encoded by the same gene, as deletion of the *TNFSF13* gene by CRISPR–Cas9 in U937 cells resulted in the loss of both nc-APRIL and c-APRIL proteins in the supernatant (Extended Data Fig. 8o, p). In addition, both nc-APRIL and c-APRIL can be produced by the same transcript, as transfection of 293T cells with a plasmid containing a cDNA for wild-type human APRIL linked to an Fc region (Fc–APRIL) led to the production of both nc-APRIL and c-APRIL in the supernatant (Fig. 4d, e). We then characterized purified human recombinant nc-APRIL and c-APRIL by 'bottom-up' MS-based proteomics and found two different C-terminal tryptic peptides: an abundant one from which the C-terminal leucine residue was released by trypsin, and a minor one in which the C-terminal leucine was still attached. Although most tryptic peptide fragments were equally abundant for c-APRIL and nc-APRIL, the miscleaved fragment was not detectable in nc-APRIL by high-sensitivity targeted parallel reaction monitoring, suggesting that the C terminus of nc-APRIL might have already been truncated (Extended Data Fig. 9a–c, Supplementary Table 1). As the C terminus of APRIL is structurally important (Extended Data Fig. 9d), we investigated the effect of C-terminal amino acid truncations in determining the ratio of c-APRIL to nc-APRIL. We transfected Fc–APRIL with a C-terminal truncation of one amino acid (–1C) into 293T cells, which led to the exclusive production of nc-APRIL in the supernatant; cells transfected with wild-type Fc–APRIL contained both c- and nc-APRIL (Fig. 4d, e). Similar data were obtained with C-terminal truncations of two, three or four amino acids (Fig. 4d, e). Nc-APRIL proteins that were produced following truncations of between one and four amino acids also did not bind the receptor BCMA (Fig. 4f), which is consistent with nc-APRIL lacking the TACI-binding site (Extended Data Fig. 8i). Nc-APRIL is present at higher levels than c-APRIL in human serum (Fig. 4g, Supplementary Fig. 1). Together, these data indicate that different forms of APRIL exist in vivo. As c-APRIL and nc-APRIL could be also formed from the same wild-type amino acid sequence, APRIL may belong to the group of metamorphic proteins—proteins that switch between different folding states[18].

Next, we quantified serum nc-APRIL and c-APRIL levels in 785 individuals from the prospective ICARAS study[19] with neurologically asymptomatic carotid atherosclerosis (Supplementary Table 2a). Kaplan–Meier analyses showed that decreasing serum nc-APRIL levels were associated with a significant increase in cardiovascular and all-cause mortality, even after adjustment for traditional cardiovascular risk factors (Fig. 4h, Extended Data Table 1a, Supplementary Table 2b). By contrast, serum c-APRIL levels were not associated with cardiovascular or all-cause mortality (Extended Data Table 1b). Moreover, we quantified nc-APRIL levels in the serum of 1,514 patients from the prospective LURIC study[20] who had symptomatic and angiographically documented coronary artery disease (Supplementary Table 3a). Kaplan–Meier analyses demonstrated a statistically significant increase in cardiovascular mortality with increasing serum nc-APRIL levels in a follow-up ten years after recruitment to the study (Fig. 4i, Supplementary Table 3b), even after adjustment for multiple well-established cardiovascular risk factors (Extended Data Table 1c). Similar results were obtained for all-cause mortality (hazard ratio 1.15, 95% confidence interval (CI) 1.05–1.25, $P = 0.002$). We also show that high levels of nc-APRIL in the serum of 974 patients with acute myocardial infarction (from the FAST-MI clinical study[21]) were independently associated with death two years after myocardial infarction (Extended Data Table 1d).

The differential directionality in patients with symptomatic disease or acute myocardial infarction may reflect the advanced disease stage or acute setting, respectively. These data show that circulating nc-APRIL levels are independently associated with cardiovascular mortality in three clinical studies and thereby provide epidemiological evidence for the relevance of APRIL to human atherosclerotic cardiovascular disease.

In conclusion, we show that APRIL confers atheroprotection by binding to heparan sulfates in the arterial intima. It is likely that the stoichiometric relationship of this interaction may change and be modulated by additional factors (such as chemokines reacting with heparan sulfate chains) as atherosclerotic cardiovascular disease progresses. Future studies will investigate the therapeutic value of targeting APRIL in atherosclerotic cardiovascular disease.

Online content

Any methods, additional references, Nature Research reporting summaries, source data, extended data, supplementary information, acknowledgements, peer review information; details of author contributions and competing interests; and statements of data and code availability are available at https://doi.org/10.1038/s41586-021-03818-3.

1. Libby, P. The changing landscape of atherosclerosis. *Nature* **592**, 524–533 (2021).
2. Gisterå, A. & Hansson, G. K. The immunology of atherosclerosis. *Nat. Rev. Nephrol.* **13**, 368–380 (2017).
3. Ingold, K. et al. Identification of proteoglycans as the APRIL-specific binding partners. *J. Exp. Med.* **201**, 1375–1383 (2005).
4. Vincent, F. B., Morand, E. F., Schneider, P. & Mackay, F. The BAFF/APRIL system in SLE pathogenesis. *Nat. Rev. Rheumatol.* **10**, 365–373 (2014).
5. Castigli, E. et al. Impaired IgA class switching in APRIL-deficient mice. *Proc. Natl Acad. Sci. USA* **101**, 3903–3908 (2004).
6. Huard, B. et al. APRIL secreted by neutrophils binds to heparan sulfate proteoglycans to create plasma cell niches in human mucosa. *J. Clin. Invest.* **118**, 2887–2895 (2008).
7. McCarron, M. J., Park, P. W. & Fooksman, D. R. CD138 mediates selection of mature plasma cells by regulating their survival. *Blood* **129**, 2749–2759 (2017).
8. Hymowitz, S. G. et al. Structures of APRIL-receptor complexes: like BCMA, TACI employs only a single cysteine-rich domain for high affinity ligand binding. *J. Biol. Chem.* **280**, 7218–7227 (2005).
9. Sandberg, W. J. et al. The tumour necrosis factor superfamily ligand APRIL (TNFSF13) is released upon platelet activation and expressed in atherosclerosis. *Thromb. Haemost.* **102**, 704–710 (2009).
10. Lord, M. S. et al. The multifaceted roles of perlecan in fibrosis. *Matrix Biol.* **68-69**, 150–166 (2018).
11. Tran-Lundmark, K. et al. Heparan sulfate in perlecan promotes mouse atherosclerosis: roles in lipid permeability, lipid retention, and smooth muscle cell proliferation. *Circ. Res.* **103**, 43–52 (2008).
12. Sarrazin, S., Lamanna, W. C. & Esko, J. D. Heparan sulfate proteoglycans. *Cold Spring Harb. Perspect. Biol.* **3**, a004952 (2011).
13. Parish, C. R. The role of heparan sulphate in inflammation. *Nat. Rev. Immunol.* **6**, 633–643 (2006).
14. Bernelot Moens, S. J. et al. Impact of the B cell growth factor APRIL on the qualitative and immunological characteristics of atherosclerotic plaques. *PLoS One* **11**, e0164690 (2016).
15. Haselmayer, P., Vigolo, M., Nys, J., Schneider, P. & Hess, H. A mouse model of systemic lupus erythematosus responds better to soluble TACI than to soluble BAFFR, correlating with depletion of plasma cells. *Eur. J. Immunol.* **47**, 1075–1085 (2017).
16. Tsiantoulas, D. et al. B cell-activating factor neutralization aggravates atherosclerosis. *Circulation* **138**, 2263–2273 (2018).
17. Tsiantoulas, D. et al. Increased plasma IgE accelerate atherosclerosis in secreted IgM deficiency. *Circ. Res.* **120**, 78–84 (2017).
18. Dishman, A. F. et al. Evolution of fold switching in a metamorphic protein. *Science* **371**, 86–90 (2021).
19. Schillinger, M. et al. Inflammation and Carotid Artery—Risk for Atherosclerosis Study (ICARAS). *Circulation* **111**, 2203–2209 (2005).
20. Winkelmann, B. R. et al. Rationale and design of the LURIC study—a resource for functional genomics, pharmacogenomics and long-term prognosis of cardiovascular disease. *Pharmacogenomics* **2** (Suppl 1), S1–S73 (2001).
21. Puymirat, E. et al. Acute myocardial infarction: changes in patient characteristics, management, and 6-month outcomes over a period of 20 years in the FAST-MI program (French Registry of Acute ST-Elevation or Non-ST-Elevation Myocardial Infarction) 1995 to 2015. *Circulation* **136**, 1908–1919 (2017).

Methods

Mice, treatments and diets

Ldlr$^{-/-}$ and *Apoe*$^{-/-}$ mice were bought from The Jackson Laboratories (USA). *Tnfsf13*$^{-/-}$ mice were provided by Genentech (USA). *Bcma*$^{-/-}$ mice were provided by Biogen (USA). *Ldlr*$^{-/-}$*Tnfsf13*$^{-/-}$ mice were generated by crossing *Ldlr*$^{-/-}$ and *Tnfsf13*$^{-/-}$ mice. *Hspg2*^{d3} sperm was purchased from the Biocentre Oulu (University of Oulu) and mice were generated by in vitro fertilization of *Apoe*$^{-/-}$ mice. All mice were on a C57BL/6J background and were maintained in the SPF facility of the Medical University of Vienna (Austria), or the University of Cambridge (United Kingdom) or the University of Lausanne (Switzerland). Female *Ldlr*$^{-/-}$*Tnfsf13*$^{-/-}$ and *Ldlr*$^{-/-}$*Tnfsf13*$^{+/+}$ littermate mice (13–15 weeks old) were fed an atherogenic diet (0.2% cholesterol, 21% fat; E15721-347 bought from Ssniff, Germany) for 10 weeks. For bone marrow transplant experiments, male *Ldlr*$^{-/-}$ mice (10 weeks old) were irradiated (10.5 Gray) then reconstituted by intravenous (i.v.) injection with 7×10^6 bone marrow cells isolated from *Bcma*$^{+/+}$ and *Bcma*$^{-/-}$ donors. All mice were allowed to recover for four weeks and then they were placed on an atherogenic diet for ten weeks. Female *Apoe*$^{-/-}$ mice (8 weeks old) were injected intraperitoneally biweekly for 10 weeks with 5 mg/kg of a mixture consisting of anti-mouse APRIL antibody (Apry-1-1; AG-27B-0001PF, purchased from Adipogen, Liestal, Switzerland) and control-Ig (anti-APRIL group), or TACI-Ig and isotype IgG2b (LEAF; Biolegend) (TACI-Ig group), or isotype IgG2b and control-Ig (control group) (all reagents from Merck KGaA, Germany). In addition, all *Apoe*$^{-/-}$ mice were fed an atherogenic diet for the last 8 weeks of the study. Female littermate *Apoe*$^{-/-}$*Hspg2*^{wt} (data from *Apoe*$^{-/-}$*Hspg2*$^{wt/wt}$ and *Apoe*$^{-/-}$*Hspg2*$^{wt/d3}$ mice were pooled because no differences were observed between the two genotypes) and *Apoe*$^{-/-}$*Hspg2*^{d3} mice (8 weeks old) were injected biweekly for 7 weeks with 5 mg/kg of a either a blocking mouse anti-mouse APRIL antibody (108; Extended Data Fig. 5a–c; available from Adipogen under Centotto-1; AG-20B-0083) or an isotype IgG1 (Ultra LEAF; Biolegend), and mice were fed an atherogenic diet for the last 6 weeks of the study.

Multimeric human and mouse Flag–ACRP30–APRIL fusion proteins (referred to as Flag–APRIL) were from Adipogen (human: AG-40B-0017-C010, mouse: AG-40B-0089-C010). Wild-type C57BL/6J mice were injected intraperitoneally with either 1 µg mouse multimeric Flag–APRIL (Adipogen) or a mixture of 1 µg Flag–APRIL and 10 µg mouse anti-APRIL antibody (Apry-1-1, AG-27B-0001PF, Adipogen) in Dulbecco's phosphate-buffered saline (PBS; DPBS). Blood was collected one, three, and six hours later and Flag–APRIL was quantified as described below.

Mice were matched for sex and age in all studies. All experimental studies were approved by the Animal Ethics Committee of the Medical University of Vienna (Austria; 66.009/0281-/WFV/3b/2014, 66.009/0223-WF/II/3b/2014 and 66.009/0398-V/3b/2019) or have been regulated under the Animals (Scientific Procedures) Act 1986 Amendment Regulations 2012 following ethical review by the University of Cambridge Animal Welfare and Ethical Review Body (PPL PA4BDF775). No statistical methods were used to predetermine sample size. Mice were randomized for the treatments they received within the genotype groups.

Anti-APRIL antibodies and biologicals

Anti-hAPRIL antibodies Mahya-1 (mouse IgG1, AG-20B-0078PF-C100), 110 (mouse IgG1) and His-tagged BAFF 60-mer (AG-40B-0112-C010) were provided by Adipogen. Aprily1, Aprily2, Aprily3, Aprily5, Aprily6, Aprily8, Aprily9 and Aprily10 (mouse IgG1) were custom-made by NanoTools (Teningen, Germany). Anti-EDA antibody EctoD1 (mIgG1) was described previously[22]. The hybridoma for anti-rat SHH-5E1 (mouse IgG1) developed by T. M. Jessell and S. Brenner-Morton was obtained from the Developmental Studies Hybridoma Bank, maintained at the University of Iowa. Atacicept (TACI-Fc) was provided by Merck (KGaA). Etanercept (TNFR2-Fc) was purchased from the pharmacy of Lausanne University Hospital (CHUV). Bovine serum albumin was from Thermo Scientific (cat no. 23209).

Quantification of size, necrotic core and collagen content of atherosclerotic lesions

Atherosclerotic lesion size (staining with H&E), necrotic core content (staining with H&E or DAPI) and collagen content (staining with Sirius Red) were evaluated by computer-assisted image analysis using Adobe Photoshop Elements 6.0 and Fiji software in aortic root paraffin-embedded ($n = 9$ per mouse) or OCT-preserved cross-sections ($n = 6$ per mouse) with 50 or 80 µm distance, respectively, that were collected starting with the appearance of all three valve leaflets as described previously[16]. Data analysis was conducted in a blinded manner where appropriate.

Quantification of total cholesterol and triglycerides in mouse plasma

EDTA blood was collected from the vena cava at the time of death in MiniCollect purple cap TUBE (Greiner Bio-One). Blood was centrifuged at 1,000*g* for 20 min at room temperature. Plasma total cholesterol and triglycerides were measured in an ISO 15189-accredited medical laboratory on Beckman Coulter AU5400 (Beckman Coulter) or Roche Cobas 8000 (Roche) instruments.

Flow cytometry

Flow cytometry analysis of splenic and peritoneal B cell subsets was performed as described previously[16,17] using directly conjugated antibodies on single-cell suspensions of freshly isolated spleens and peritoneal cells. Follicular/transitional stage 2 (FO/T2; CD21$^+$CD23$^+$), marginal zone (MZ; CD21^{high}CD23$^-$), CD21$^+$CD23$^-$, transitional stage 1 (T1; CD21^{low}CD23$^-$) and newly formed (NF; CD21$^-$CD23$^-$) B cells were gated within B220$^+$CD43$^-$ cells. B-1 B cells were defined as B220^{low}IgM$^+$CD43$^+$. Splenic T cells were identified using anti-CD3 PE (clone 145-2C11; eBiosciences), anti-CD4 FITC (clone GK1.5; eBiosciences) and anti-CD8 APC (clone 53-6.7; eBiosciences). Peripheral blood from the vena cava was diluted with PBS + 2% dextran (Sigma) and incubated for at least 30 min at 37 °C to concentrate the RBCs at the bottom of the tube. The upper clear phase was collected, and cells were incubated with blocking anti-CD16/32 antibody (clone 93; eBiosciences). Peripheral monocytes were identified by staining with anti-CD11b-APC (clone M1/70; eBiosciences), anti-Ly6C-FITC (clone HK1.4; Biolegend) and anti-Ly6G-PE (clone 1A8; Biolegend) as described previously[16].

HUVECs were stained in DPBS (Sigma) supplemented with 10% FBS (Gibco) with 0.5 µg/ml of either mouse Flag-tagged APRIL[3] or amino-terminal Flag-tagged bacterial alkaline phosphatase (BAP) fusion protein (Sigma) for 30 min at 4 °C, followed by staining with 1 µg/ml of anti-flag M2 antibody (Sigma) for 20 min at 4 °C. Then cells were stained with 1 µg/ml of a biotinylated rat anti-mouse IgG1 (cloneA85-1; BD Biosciences) for 20 min at 4 °C and with streptavidin-APC (eBiosciences) for 20 min at 4 °C.

HEK293 wild-type cells were stained for 20 min on ice with 50 µl of Flag–ACRP–mAPRIL A88 (DYKDDDDKGPGQVQLH-[aa 18–111 of mACRP30]-LQ-[aa 88–232 of mAPRIL]) in FACS buffer (PBS + 5% FCS) at 1,000 ng/ml final and fivefold dilutions, either alone or after preincubation with Apry-1-1 at 25 µg/ml, or after preincubation with liquemine (DrossaPharm, Basel, Switzerland) at 10 IU/ml final concentration. Then cells were stained with biotinylated anti-Flag M2 (1:500; Sigma F9291) followed by PE-coupled streptavidin (1:500; eBiosciences).

HEK293 wild-type cells were stained with 5% rat serum in PBS + 0.5% BSA (buffer) for 15 min on ice. After washing with buffer, cells were incubated with 1, 3 or 6 µg/ml of Fc–hAPRIL-A88 for 30 min on ice. After washing, cells were incubated with human native LDL (generated as described previously[23]) at 25 or 75 or 225 µg/ml for 30 min on ice. Then, cells were incubated with 4% PFA for 20 min at room temperature. After washing with buffer, cells were stained with the monoclonal MB47 antibody (provided by the Witztum laboratory, UCSD) at 0.5µg/ml for 20 min on ice, followed by an anti-mIgG2a-biot (rat; clone R19-15; BD) for 15 min on

ice and PE-coupled streptavidin for 15 min on ice (1:400; eBiosciences). Data were acquired on a FACS Calibur (BD) or FACS Accuri C6 (BD) or LSRFortessa (BD) and were analysed using FlowJo software 7.6 (Tree Star).

Total antibody quantification in plasma by ELISA

Total IgM, IgG1, IgG2b, IgG2c, IgG3 and IgA antibodies in plasma were measured by ELISA. In brief, 96-well white round-bottomed MicroFluor microtitre plates (Thermo Lab systems) or immunoGrade, 96-well, PS Standard plates (781724; Brand) were coated with an anti-mouse IgM (Sigma; M8644; at 2 µg/ml), anti-mouse IgG1 (Biolegend; RMG1-1; at 2 µg/ml), anti-mouse IgG2b (BD Biosciences; R9-91; at 3 µg/ml), anti-mouse IgG2c (STAR135; at 1 µg/ml), anti-mouse IgG3 (BD Biosciences; R2-38; at 4 µg/ml) or anti-mouse IgA (BD Biosciences; C10-3; at 3 µg/ml) in PBS overnight and then washed three times with PBS and blocked with Tris-buffered saline containing 1% BSA (TBS/BSA) for 1 h at room temperature. Then wells were washed with either PBS (plates for IgM, IgG2b and IgG2c) or PBS supplemented with 0.05% Tween (plates for IgG1, IgG3 and IgA), and diluted mouse plasma was added in TBS/BSA to the wells and incubated overnight at 4 °C. Plates were washed, and bound Igs were detected with an anti-mouse IgM antibody conjugated to alkaline phosphatase (Sigma; A9688), the biotinylated forms of anti-mouse IgG1 (BD Biosciences; A85-1) or anti-mouse IgG2b (BD Biosciences; R12-3), anti-mouse IgG2c (JIR 115-065-208), anti-mouse IgG3 (BD Biosciences; R40-82) or anti-mouse IgA (BD Biosciences; C10-1). Wells were washed again as before and neutravidin conjugated to alkaline phosphatase was added where appropriate. Then, wells were washed again as before and rinsed once with distilled water, and 25 µl of a 30% LumiPhos Plus solution in dH_2O (Lumigen Inc.) was added. After 75 min, the light emission was measured with a Synergy 2 luminometer (BIO-TEK) and expressed as RLU per 100 ms.

For antibody isotyping, ELISA plates were coated with purified antibodies at 2 µg/ml in PBS, blocked, and incubated with horse radish peroxidase-coupled anti-IgA (#1040-05), anti-IgM (#1020-05), anti-IgG1 (#1070-05), anti-IgG2a (#1080-05), anti-IgG2b (#1090-05) or anti-IgG3 (#1100-05) (all from Southern Biotech) at 1:4,000 in ELISA buffer for 1 h at 37 °C and developed with *o*-phenylenediamine (OPD)–H_2O_2 substrate (Sigma-Aldrich, P9187). The reaction was terminated with acid and plates were read at 492 nm.

Flag–APRIL quantification by ELISA

To quantify Flag–APRIL in plasma, ELISA plates (maxi-sorp NUNC) were coated with 2 µg/ml in 70 µl final volume of an anti-Flag antibody (Biolegend; clone L5) overnight at 4 °C. Thereafter, wells were blocked with PBS + 1% BSA for 1 h at room temperature. Plasma samples were added to the wells and incubated for 2 h at room temperature. Bound Flag–APRIL was detected with a mouse anti-APRIL biotinylated antibody (clone 2C8; Extended Data Fig. 5a, b, d) used at 1 µg/ml and incubated for 1 h at room temperature. Then streptavidin–HRP (R&D) was added to the samples for 30 min at room temperature. Finally, 3,3′,5,5′ tetramethylbenzidine was added for 15 min. The reaction was terminated with acid and optical density was measured at 450 nm in a luminometer VICTOR X3 (PerkinElmer).

To quantify the interaction of APRIL with HSPG2, ELISA plates (maxi-sorp NUNC) were coated with 1 µg/ml of HSPGs from the basement membrane of Engelbreth-Holm-Swarm mouse sarcoma (Sigma) overnight at 4 °C. Thereafter, wells were blocked with PBS + 1% BSA for 1 h at room temperature and mouse multimeric Flag–APRIL (AG-40B-0089, Adipogen) was added at 1 µg/ml for 2 h at room temperature. Bound Flag–APRIL was detected with an anti-Flag conjugated to FITC (Sigma, clone: M2). Fluorescence was measured in a luminometer VICTOR X3 (PerkinElmer).

Immunofluorescence analysis

Primary HUVECs were cultured in EGM-2 Bullet kit Endothelial Cell Growth Medium without heparin (Lonza) in chambered coverslips (Ibidi) until a confluent monolayer was formed. Then cells were washed with PBS with Ca^{2+} once and fixed with 4% paraformaldehyde for 20 min. Then cells were carefully washed three times with DPBS (Sigma) and were incubated with 50 mM ammonium chloride for 10 min at room temperature. After washing as above, cells were incubated with 0.5 µg/ml of human or mouse multimeric Flag–APRIL (Adipogen). For competition experiments, staining with Flag–APRIL was also performed in the presence of 5 IU/ml heparin (National Veterinary Services LTD, UK). An anti-Flag antibody (clone: M2; Sigma) conjugated to FITC was used to detect Flag–APRIL.

Paraffin-embedded sections of human coronary and carotid artery specimens with or without atherosclerotic plaques obtained at necropsy and anonymized were provided by Patrick Bruneval (Paris Transplant Group, France). Sections were rehydrated by incubation first in xylene (three times; each three minutes), then in ethanol (100%, 96%, 90% and 70%; each for three minutes) and finally in dH_2O for three minutes. Then antigen retrieval (Dako) was performed for 1 h in a water bath at 100 °C. Sections were then permeabilized in 0.1% Triton + citric acid for 20 min and were blocked with 5% goat and/or donkey serum diluted in assay buffer (PBS + 2.5% BSA + 2 mM EDTA + 0.01% sodium azide) for 30 min. Sections were then stained with mouse anti-human APRIL (Aprily-2), anti-HSPG2 (clone: A7L6; Merck Millipore) and anti-CD31 (clone: EPR3094; Abcam) antibodies in blocking buffer overnight at 4 °C. Next, sections were stained with goat anti-rat AF488, goat anti-rabbit AF647 and goat anti-mouse AF555 or goat anti-mouse AF488 and donkey anti-rat AF555 (all from Life Technologies) where appropriate, in assay buffer for 3 h at room temperature.

Paraffin-embedded sections of mouse aortic root with atherosclerotic plaques were rehydrated by incubation first in xylene (three times; each 3 min), then in ethanol (100%, 96%, 90% and 70%; each for 3 min) and finally in dH_2O for 3 min. Then antigen retrieval (Dako) was performed for 1 h in a water-bath at 100 °C. Sections were blocked with 5% donkey serum or a mixture of 5% mouse serum and 2.5 µg/ml of anti-mouse CD16/32 antibody (clone 93; Invitrogen) diluted in assay buffer (PBS + 2.5% BSA + 2 mM EDTA + 0.01% sodium azide) for 30 min. Sections were then stained with rat anti-mouse Mac-2 (M3/38; Biolegend), rabbit polyclonal anti-ApoB (ab20737; Abcam), or mouse anti-aSMC antibody conjugated to Cy-3 (clone 1A4; Sigma) in blocking buffer overnight at 4 °C. Next, sections were stained with either donkey anti-rat AF488 or donkey anti-rabbit AF555 (all from Life Technologies) in assay buffer for 3 h at room temperature.

For the LDL binding competition assay, cryosections (10 µm thickness) of a sham-operated mouse carotid artery from a model of neointima hyperplasia as described previously[24] were fixed in acetone for 20 min at −20 °C and then were incubated with 10 µg/ml of mouse multimeric Flag–APRIL in assay buffer (PBS + 2.5% BSA + 2 mM EDTA + 0.01% sodium azide) or only with assay buffer overnight at 4 °C. After washing in DPBS (Sigma), sections were incubated with 100 µg/ml of human native LDL (isolated from healthy donors) for two hours at room temperature. Sections were then fixed in 4% PFA for 15 min at room temperature and then blocked with 5% donkey serum in assay buffer. Sections were then stained with a rabbit anti-ApoB antibody (Abcam; ab20737) for 1.5 h at room temperature and then with a donkey anti-rabbit conjugated to AF555 (Life Technologies) for 1 h at room temperature.

Mouse multimeric Flag–APRIL was detected with an anti-Flag PE (Biolegend; clone: L5) or a mouse anti-mouse APRIL biotinylated antibody (clone: 2C8) and streptavidin PE (Biolegend) in sections that were blocked with 5 µg/ml of anti-CD16/32 antibody (Thermo Fisher Scientific; clone: 93). For competition experiments with heparin, Flag–APRIL was mixed with 30 IU/ml heparin (National Veterinary Services LTD, UK) before being added to the section.

HSPG2 in mouse carotid arteries was detected with an anti-HSPG2 antibody (clone: A7L6; Merck Millipore) and donkey anti-rat AF555 (Life Technologies). Finally, all samples were stained with Hoechst or DAPI

solution for 8 min at room temperature. Epifluorescence or confocal microscopy were performed using a Leica CTR6500 or Axio Imager M2 or Carl Zeiss LSM 700 (ZEISS) or LSM780 (ZEISS) microscope and Zen software. The Fiji software was used for image analysis[26]. The plugin JACoP in Fiji was used to calculate Pearson's coefficient. The antibodies were used at 1–6 µg/ml where appropriate.

Coupling of proteins to Sepharose beads

Five milligrams of TACI-Fc or TNFR2-Fc, or 2 mg of Aprily1, Aprily2[3], Aprily3, Aprily5, Aprily6, Aprily8, Aprily9 or Aprily10 or EctoD1 antibodies or mouse IgG1 5E1 anti-rat SHH were coupled to 1 ml of NHS-activated Sepharose beads (GE Healthcare, #90-1004-00). In brief, beads stored in isopropanol were centrifuged for 5 min at 2,400*g* and washed three times with 1 ml ice-cold 1 mM HCl. One millilitre of TACI-Fc or TNFR2-Fc at 5 mg/ml or Aprily or anti-rat SHH antibodies at 2 mg/ml in 0.2 M $NaHCO_3$, 0.5 M NaCl, pH 8.3 was added to the beads and incubated for 30 min at room temperature. Beads were then washed three times with 1 ml ethanolamine buffer (0.5 M ethanolamine, 0.5 M NaCl, pH 8.3) and then three times with 1 ml acetate buffer (0.1 M sodium acetate, 0.5 M NaCl, pH 4) and again with 3 ml ethanolamine buffer. Beads were incubated for 30 min at room temperature in ethanolamine buffer, then washed three times with acetate buffer, then ethanolamine buffer, then acetate buffer and finally PBS. Beads were stored in 1 ml PBS 0.05% azide at 4 °C.

Production and quantification of Flag-tagged or Fc-tagged APRIL

Flag–hAPRIL, Flag–mAPRIL, Flag–mAPRIL (+Ala112) or Fc–hAPRIL with deletion or truncations at the C terminus were transiently transfected in 293T cells using PEI[25] in serum-free OptiMEM medium in 10-cm plates. After seven days, the supernatants of Fc-tagged constructs were collected, and the cells were washed in PBS and lysed in 200 µl SDS containing lysis buffer plus DTT and boiled for 5 min at 95 °C to be loaded on a SDS–PAGE. Also, seven days after the transfection, the supernatants of Flag-tagged APRIL constructs were affinity-purified on TACI-Fc-Sepharose (see section 'Coupling of proteins to Sepharose beads'), eluted with 50 mM of Na-citrate pH 2.7 and immediately neutralized with Tris-HCl pH 9. Buffer was exchanged for PBS using a 30 kDa cut-off centrifugal device (Millipore). Purified proteins were quantified by absorbance at 280 nm using 1 mg/ml extinction coefficients of 0.857 and 1.092 for Flag–hAPRIL and Flag–mAPRIL respectively. The concentration of Flag–hAPRIL was also determined by densitometric quantification using Fiji software[26] of Coomassie-blue-stained SDS–PAGE gels using His–BAFF and bovine serum albumin (BSA) as standards. C-APRIL was produced by affinity purification of conditioned supernatants containing Flag–hAPRIL on TACI-Fc-Sepharose beads, followed by depletion on Aprily2-Sepharose beads. Conversely, nc-APRIL was affinity purified on Aprily2-Sepharose beads followed by depletion on TACI-Fc-Sepharose beads. Denatured Flag–hAPRIL was prepared by mixing 1 µg purified Flag–hAPRIL with 1 µl denaturation buffer from a PNGase F kit (Biolabs, P0704S lot: 0431703) and 8 µl H_2O, and heating for 10 min at 100 °C. Then the mix was neutralized with 2 µl of 10% NP-40 and 2 µl of 10 × glyco-buffer 2 from the same kit.

Size-exclusion chromatography

One hundred nanograms of Adipogen APRIL (h) ELISA kit standard, which was depleted either on TACI-Fc- or Aprily2-Sepharose beads and their eluates, were size-fractionated at a flow rate of 0.7 ml/min on a Superdex S200 Increase HR 10/30 column (GE Healthcare) equilibrated in PBS, 10 µg/ml BSA, with online absorbance monitoring at 280 nm and 1 ml fraction collection. Fractions were tested in Adipogen and Invitrogen ELISA kits. The column was calibrated with 100 µl of a mixture of the following proteins, each at 1.4 mg/ml, except ferritin at 0.14 mg/ml, with sizes of: 669 (thyroglobulin), 440 (ferritin), 158 (aldolase), 13.7 (RNase A), all from GE Healthcare), 67 (bovine serum albumin), 43 (ovalbumin), 29 (carbonic anhydrase), and 6.5 kDa (aprotinin) (all from Sigma-Aldrich).

SDS–PAGE

SDS–PAGE and western blot (using Aprily2 at 0.5 µg/ml) were performed under reducing conditions according to standard procedures and revealed using WesternBright ECL spray (Advansta). Coomassie blue staining was performed with a semidry iD Stain System (Eurogentech).

HEK293T, HEK293, Jurkat BCMA–Fas-2309 cl13 and U937 cells

HEK293T, HEK293 and histiocytic lymphoma U937 cells were obtained from the late Jürg Tschopp (University of Lausanne). HEK293T cells were cultured in DMEM plus 10% fetal calf serum. Jurkat BCMA–Fas-2309 cl13 cells were cultured in RPMI plus 10% fetal calf serum as reported previously[27]. U937 cells and U937 cells deficient for BAFF were described previously[28]. U937 cells deficient for APRIL or deficient for BAFF and APRIL were generated by lentiviral transduction of a CRISPR–Cas9-expression vector carrying a hAPRIL guide RNA (gRNA) as described[28], except that the following annealed oligonucleotides were used for cloning (5′-CACCGAGGATATGGTGTCCGAATCC-3′ and 5′- AAACGGATTCGGACACCATATCCTC-3′). U937 cells were cultured in RPMI supplemented with 10% fetal calf serum. None of the cell lines has been authenticated. All cell lines tested negative for mycoplasma. HEK293 and HEK293T cells are included in the ICLAC and NCBI biosample list. The justification to use HEK293 cells is that as long as they bind APRIL in a heparin-inhibitable manner, the cell type does not affect the assays included in our studies. The justification for 293T cells is that as long as they express the transfected proteins, the cell type does not affect the assays included in our studies.

HUVEC culture

Primary HUVECs were provided by Marion Gröger (Medical University of Vienna, Austria) or Sanjay Sinha's group (University of Cambridge, UK). Cells were cultured in either EGM-2 Bullet kit Endothelial Cell Growth Medium without heparin (Lonza) or IMDM supplemented with 10% FBS, 1% glutamine, 1% Pen-Strep and 2% LSGS (Gibco). Cells were used up to the fifth passage.

Human umbilical artery smooth muscle cells

Human umbilical artery smooth muscle cells were a gift from Peter Petzelbauer's laboratory (Medical University of Vienna, Austria). Cells were cultured in Smooth Muscle Cell Growth Medium 2 (Promocell). For gene expression analysis, cells were cultured in 24-well plates (ThermoFisher) until 80–90% confluency and then were stimulated with human TNF (eBiosciences) at 100 ng/ml, native human LDL at 50 µg/ml or CuOx-LDL at 50 µg/ml for 4 h. Native human LDL (isolated from healthy donors) and CuOx-LDL were generated as described previously[23].

Cytotoxicity assay

Cytotoxicity assays using BCMA–Fas cells were performed as described[29]. In brief, flat-bottomed 96-well plates with $3–4 \times 10^4$ reporter cells per well in a final volume of 100 µl RPMI plus 10% fetal calf serum were used in the presence of the indicated concentrations of Flag–hAPRIL or Flag–mAPRIL, and 100 ng/ml of TACI-Fc, Apry-1-1 or monoclonal antibody (mAb) 108. For mock experiments, the same volume as truncated APRIL was used. After an overnight incubation at 37 °C, 5% CO_2, cell viability was monitored with a colorimetric (PMS/MTS) test.

Total RNA extraction, cDNA synthesis and real-time PCR analysis

Total RNA was extracted from cells with the peqGold total RNA kit (Peqlab) and cDNA was synthesized using the high-capacity cDNA reverse transcription kit (Applied Biosystems). Quantitative real-time SYBR green-based PCR (Peqlab) was performed with the KAPA SYBR green FAST BioRad icycler kit (Peqlab) on a BioRad CFX96 real-time

system. *36B4* and *18S* were used as reference genes. Data were analysed using the ddCT method.

Primer list

mouse *Bcma* forward: 5- ATCTTCTTGGGGCTGACCTT-3
mouse *Bcma* reverse: 5- CTTTGAGGCTGGTCCTTCAG -3
36B4 forward: 5-AGGGCGACCTGGAAGTCC-3
36B4 reverse: 5-CCCACAATGAAGCATTTTGGA-3
human *TNFSF13* forward: 5- ATGGGTCAGGTGGTGTCTCG-3
human *TNFSF13* reverse: 5-TCCCCTTGGTGTAAATGGAAGA-3
human *IL6* forward: 5- CAGGAGAAGATTCCAAAGAT-3
human *IL6* reverse: 5- CTCTTGTTACATGTCTCCTT-3
human *18S* forward: 5- GTAACCCGTTGAACCCCATT-3
human *18S* reverse: 5- CCATCCAATCGGTAGTAGCG-3

RNA sequencing and data analysis

Aortas were isolated from C57BL/6 male mice. For ex vivo samples, tissues were immediately transferred to RNAlater followed by isolation of ascending aorta (AA) and descending thoracic aorta (DT) segments before manual removal of the adventitial and endothelial cell layers. The cleaned medial layer from 3–5 animals was then lysed in Trizol (Thermo-Fisher), RNA isolated and cleaned on a RNeasy column (Qiagen). In vitro cultured vascular smooth muscle cell (VSMC) samples were isolated from enzymatically dispersed VSMCs that had been cultured for 4–5 passages in DMEM supplemented with 10% fetal calf serum, glutamine and penicillin. Sequencing libraries were generated from 550 ng quality-assessed total RNA (RNA integrity number (RIN) 7.8–9) using the TruSeq Stranded mRNA Library Prep Kit (Illumina) and sequenced using HiSeq (Illumina).

For data analysis, raw sequencing reads were quality controlled using FastQC v0.11.3 (https://www.bioinformatics.babraham.ac.uk/projects/fastqc/) and trimmed using the Trim Galore v0.4.1 wrapper (https://www.bioinformatics.babraham.ac.uk/projects/trim_galore/). Reads were then aligned to the GRCm38 mouse reference genome using Tophat v2.0.12. Reads with a minimum map quality of 20 were imported into Seqmonk 1.45.4 (http://www.bioinformatics.babraham.ac.uk/projects/seqmonk) for quantification using the RNA-seq quantification pipeline, and visualization. Data are available from the GEO under accession numbers GSE117963 (from VSMCs from the aortic arch and descending thoracic aorta) and GSE17858 (from mouse primary VSMCs that were stored in Trizol after isolation or had been cultured for 4–5 passages until the analysis).

Surface plasmon resonance

For the Biacore measurements, a Biacore X100 system was used. Biotinylated heparin at a concentration of 1.5 µg/ml (Sigma-Aldrich B9806-10MG) was coupled to a Streptavidin Sensor Chip SA (Cytiva BR100032) as the ligand, reaching a response of 152.2 RU. All measurements were performed in PBS as general buffer. The different purified proteins (analytes) were tested in a single-cycle kinetics/affinity assay, preceded by priming and a startup cycle with buffer. Protein solutions were prepared as a 3× dilution series in PBS going down from 1,000 nM (1000/333/111/37/12.3 nM), with 70 s contact time, 600 s dissociation time, and 30 s regeneration contact time. The chip was regenerated using a 500 mM NaCl, 25 mM NaOH solution. Results were analysed using the Biacore X100 Evaluation software version 2.0.1 Plus Package. Stable response was measured just before injection of the next higher concentration (150 s after injection stop, time window 15 s). K_D values were calculated using the steady-state affinity model. Values of the stable response at different concentrations were exported and plotted as a binding curve using GraphPad Prism version 8.4.0 for Mac.

Mass spectrometry, sample preparation

HUVECs. HUVECs were cultivated in 10-cm dishes in IMDM supplemented with 10% FBS, 1% glutamine, 1% Pen-Strep and 2% LSGS (Gibco) until they reached 90% confluency. Then medium was removed, and cells were stimulated (in duplicates) with 0.5 µg/ml of either mouse Flag-tagged APRIL[3] or amino-terminal Flag-tagged BAP protein (Sigma) as control bait for 30 min at 37 °C. At the end of the stimulation, cells were washed three times with DPBS (Sigma) and on-plate cell lysis was performed with immunoprecipitation buffer (50 mM Tris, 150 mM NaCl, 1% NP-40, 5 mM EDTA, 5 mM EGTA complemented with 5 mM PMSF and protease inhibitor cocktail (Sigma)) for 20 min at 4 °C. Lysates were cleared of non-lysed particles by centrifugation and protein concentration was determined by bicinchoninic acid (BCA) assay (Pierce). Seven hundred and fifty micrograms of each lysate was incubated with 20 µl of washed anti-flag M2 bead gel (Sigma) for 4 h at 4 °C with gentle rotation. Supernatants were removed, beads were washed three times with TBS and proteins were eluted twice with 100 mM glycine pH 3.0 for 5 min at room temperature. Eluates were neutralized by addition of TBS pH 7.4. After denaturation with NP-40 and incubation at 95 °C for 10 min, 1,000 units PNGase F (New England Biolabs) was added and incubated at 37 °C for 6 h. Deglycosylated proteins were subjected to tryptic digestion using the filter-aided sample preparation (FASP) protocol[30,31]. In brief, proteins were reduced with DTT, loaded onto 30 kDa molecular weight cut-off filter columns and washed with 8 M urea in 100 mM Tris. Reduced cysteine side chains were alkylated with 55 mM iodoacetamide for 30 min at room temperature in the dark. Excessive reagent was removed by additional washing steps with 8 M urea in 100 mM Tris. The buffer was exchanged again by washing with 50 mM triethylammonium bicarbonate and 1 µg sequencing grade trypsin (Promega) was added to each filter. The digest was allowed to proceed for 16 h at 37 °C. The resulting peptides were washed off the filters and desalted using the stop-and-go extraction (STAGE) protocol[32]. Desalted peptides were reconstituted in 5% formic acid for liquid chromatography with tandem mass spectrometry (LC–MS/MS) analysis.

Human APRIL. Ten micrograms (~10 µl) of purified canonical or non-canonical APRIL was resuspended in 50 µl 8M urea in 100 mM triethylamine bicarbonate (TEAB) buffer, pH 8 and proteins reduced with a final concentration of 10 mM DTT and incubated at 56 °C for 1 h. After cooling down to room temperature, reduced cysteines were alkylated with iodoacetamide at a final concentration of 55 mM for 30 min in the dark. Prior to tryptic digestion, urea concentration was diluted with 100 mM TEAB buffer pH 8 to 1.5 M and samples were digested with 1 µg trypsin overnight at 37 °C. Peptides were acidified to a final concentration of 1% TFA and cleaned up by solid phase extraction using C18 SPE columns (SUM SS18V, NEST group, USA) according to the manufacturer's instructions. Peptides were eluted using two times 50 µl 90% acetonitrile, 0.4% formic acid, organic solvent removed in a vacuum concentrator and dried samples reconstituted in 20 µl of 0.1% TFA.

One-dimensional reverse-phase LC–MS

HUVECs. LC–MS was performed on a Q Exactive Hybrid Quadrupole-Orbitrap (ThermoFisher Scientific, Waltham, MA) coupled to an Agilent 1200 HPLC nanoflow system (Agilent Biotechnologies, Palo Alto, CA) via nanoelectrospray ion source using a liquid junction (Proxeon, Odense, Denmark). Tryptic peptides were loaded onto a trap column (Zorbax 300SB-C18 5 µm, 5 × 0.3 mm, Agilent Biotechnologies) at a flow rate of 45 µl/min using 0.1% TFA as loading buffer. After loading, the trap column was switched in-line with a 75-µm inner diameter, 20-cm analytical column (packed in-house with ReproSil-Pur 120 C18-AQ, 3 µm, Dr. Maisch, Ammerbuch-Entringen, Germany). Mobile phase A consisted of 0.4% formic acid in water and mobile phase B 90% acetonitrile in water plus 0.4% formic acid. The flow rate was set to 250 nl/min and a 60-min gradient applied (4% to 24% solvent B within 30 min, 24% to 36% solvent B within 4 min and, 36% to 100% solvent B within 1 min, 100% solvent B for 4 min before equilibrating at 4% solvent B for 21 min). For the MS/MS experiment, the Q Exactive MS was operated in a Top10 DDA mode with an MS1 scan range of 350

to 1,650 *m/z* at a resolution of 70,000 (at *m/z* of 200). Automatic gain control (AGC) was set to a target of 3×10^6 and a maximum injection time of 100 ms. MS2 spectra were acquired at a resolution of 17,500 (at *m/z* of 200) with AGC settings of 1×10^5 and a maximum injection time of 120 ms. Precursor isolation width was set to 1.6 Da and the HCD normalized collision energy to 28%. The threshold for selecting MS2 precursor ions was set to an underfill ratio of ~12%. Dynamic exclusion for selected ions was 60 s. A single lock mass at *m/z* 445.120024 was used for internal mass calibration[33]. All samples were analysed in technical duplicate. XCalibur version 4.1.31.9 Tune 2.9.2926 was used to operate the Q Exactive MS instrument.

Human APRIL. Mass spectrometry was performed on an Orbitrap Fusion Lumos Tribrid mass spectrometer (Thermo Fisher Scientific, San Jose, CA) coupled to a Dionex U3000 RSLC nano UHPLC system (Thermo Fisher Scientific, San Jose, CA) via nanoflex source interface applying a hybrid approach consisting of an inclusion list-triggered data-dependent acquisition (DDA) experiment followed by a parallel reaction monitoring (PRM) experiment. A preceding DDA discovery shotgun LC–MS experiment was carried out to generate a scheduled mass list for 99 selected human Fc–APRIL-derived high-confidence (1% false discovery rate (FDR)) peptide sequences using Proteome Discoverer 2.4. Approximately equal amounts of either canonical or non-canonical APRIL tryptic peptides were loaded onto a trap column (Acclaim PepMap 100 C18, 3µm, 5 × 0.3 mm, Fisher Scientific, San Jose, CA) at a flow rate of 10 µl/min using 0.1% TFA as loading buffer. After loading, the trap column was switched in-line with a 50-cm, 75-µm inner diameter analytical column (Acclaim PepMap 100 C18, 2 µm, Fisher Scientific, San Jose, CA) maintained at 50 °C. Mobile phase A consisted of 0.4% formic acid in water and mobile phase B of 0.4% formic acid in a mix of 90% acetonitrile and 10% water. The flow rate was set to 230 nl/min and a 90-min gradient applied (4 to 24% solvent B within 82 min, 24 to 36% solvent B within 8 min and, 36 to 100% solvent B within 1 min, 100% solvent B for 6 min before re-equilibrating at 4% solvent B for 18 min). For the MS/MS (DDA) experiment, the MS was operated in a 3 s TopN-dependent scan cycle mode with an MS1 scan range of 375 to 1,650 *m/z* at a resolution of 120,000 (at *m/z* of 200). Automatic gain control (AGC) was set to a target value of 2×10^5 and a maximum injection time of 80 ms. MS2 scans were acquired at a resolution of 15,000 (at *m/z* of 200) with an AGC setting of 5×10^4 and a maximum injection time of 100 ms. Precursor isolation width was set to 1.6 Da and HCD normalized collision energy to 30%. Additional parameters were: MIPS enabled for peptide selection, intensity threshold for selecting precursor ions set to 5×10^4, charge state inclusion of 2–6 and dynamic exclusion for selected ions set to 60 s and a targeted mass list filter (scheduled mass list of 99 *m/z* values). A single lock mass at *m/z* 445.120024 was used. Settings for PRM were quadrupole isolation window *m/z* of 0.8, HCD fragmentation using 30% NCE, Orbitrap detection at a resolution of 15,000 (at *m/z* of 200) and a defined first mass of 120 *m/z*. Automatic gain control (AGC) was set to a target of 5×10^4 and a maximum injection time of 50 ms. XCalibur version 4.3.73.11 and Tune 3.3.2782.28 were used to operate the instrument.

Mass spectrometry data analysis

HUVECs. Raw files were searched against a human database (containing 42,265 entries, downloaded from SwissProt (https://www.uniprot.org/) on 30 December 2016) using Mascot version 2.3.02 (Matrix Science, London, UK) and Phenyx (GeneBio, Geneva, Switzerland) as search engines. Common contaminating proteins, such as porcine trypsin, were appended to the database. Mass tolerances were set to 4 ppm and 0.025 Da for precursor and fragment ions, respectively. Cleavage specificity was set to tryptic, however, one missed cleavage was allowed. Carbamidomethylation of cysteines was set as a static modification and oxidation of methionines was considered as a dynamic modification. A target-decoy search strategy was used to ensure an FDR of 1% on the protein level.

Human APRIL. Acquired raw data files were processed using Proteome Discoverer 2.4.1.15 SP1 for DDA experimental data or Skyline version 20.1.0.155 for PRM experimental data. A database search within PD 2.4 was done using the Sequest HT algorithm and Percolator validation software node (V3.04) to remove false positives with strict filtering at an FDR of 1% on PSM, peptide and protein levels. Searches were performed with full tryptic digestion against the human SwissProt database V2017.06 including a common contamination list with up to two miscleavage sites. Oxidation (+15.9949 Da) of methionine was set as variable modification, while carbamidomethylation (+57.0214 Da) of cysteine residues was set as fixed modification. Data were searched with mass tolerances of ±10 ppm and 0.025 Da on the precursor and fragment ions, respectively. Results were filtered to include peptide spectrum matches (PSMs) with Sequest HT cross-correlation factor (Xcorr) scores of ≥1 and high peptide confidence. For relative quantitative comparison of 26 selected APRIL tryptic peptide sequences, Skyline analysis was performed for canonical and non-canonical Fc–APRIL. The PD result file was used to build up a reference spectral library for Skyline analysis. Product ion chromatograms were extracted using the following Skyline settings: spectrum library ion match tolerance of 0.1 *m/z*; method match tolerance of 0.025 *m/z*; MS/MS filtering using targeted acquisition method at resolving power of 15,000 at *m/z* of 200. High-selectivity extraction was used for all matching scans. Integrated peak abundance values for selected peptides were exported (Supplementary Table 1).

Human blood collection from healthy individuals

Human blood was collected from fasted healthy volunteers via venipuncture of the antecubital vein using 21G needles. Blood samples were collected into 9-ml serum- or sodium citrate (3.8%)-containing collection tubes (VACUETTE tubes, Greiner Bio-One) and centrifuged within 20 min of venipuncture twice for 10 min at 2,000*g* at room temperature. All plasma and serum samples were aliquoted in 1.5-ml or 2-ml microtubes and were stored at −80 °C until further analysis. Human blood collection was conducted with the approval of the Ethics Committee of the Medical University of Vienna, Austria (EK Nr: 1845/2015).

Human APRIL quantification

Canonical APRIL (c-APRIL) in human serum was quantified with the APRIL (human) ELISA kit (Adipogen, AG-45B-0012-KI01; referred to as ELISA 1 in the main text) and non-canonical APRIL (nc-APRIL) with the APRIL Human ELISA kit (Invitrogen, BMS2008; referred to as ELISA 2 in the main text), according to the manufacturer's instructions. For ELISA validation, 100 µl of normal human serum, or 100 µl of Invitrogen APRIL standard at 12.5 ng/ml, were depleted overnight at 4 °C with 20 µl of a 50% slurry of Sepharose beads coupled to the indicated combinations of Aprily2, TACI-Ig or control reagents, with agitation. Beads were spun, and supernatants were depleted again with fresh beads. APRIL in supernatants was measured with the Invitrogen ELISA (80 µl) or with the Adipogen ELISA (10 µl for sera, 2 µl for standard). For native and unfolded APRIL, 50 µl at 5 µg/ml was depleted overnight at 4 °C with 30 µl of a 50% slurry of the indicated bead combinations, then beads were spun down and 15 µl of supernatant was analysed by western blot according to standard procedures, revealed with Aprily2 at 0.5 µg/ml, followed by horseradish peroxidase-coupled anti-mouse secondary antibody and ECL. Total APRIL in total denatured protein extracts from human atherosclerotic plaques ($n = 199$) from the Athero-Express[34] was quantified using the APRIL Human ELISA kit (Invitrogen, BMS2008).

Patients

We used data for patients from the LURIC prospective clinical study (The Ludwigshafen Risk and Cardiovascular Health study)[20], the ICARAS (Inflammation and Carotid Artery-Risk for Atherosclerosis Study)[19] and French Registry of Acute ST-elevation or non-ST-elevation Myocardial Infarction clinical study (FAST-MI)[21].

ICARAS study. In this single-centre study, 1,268 consecutive patients who underwent duplex ultrasound investigations of the extracranial carotid arteries were prospectively enrolled between March 2002 and March 2003. Of these, 203 patients (16%) were lost to clinical follow-up and for 280 patients (22%) no serum sample for the measurement of APRIL levels was available, leaving 785 patients for the final analysis. The 483 patients who had to be excluded from analysis did not differ significantly from the subjects who were included with respect to baseline and demographic parameters (age, sex, frequency of risk factors for atherosclerosis, and cardiovascular comorbidities; data not shown). The study cohort comprised 486 male patients (62.1%); the median age was 69.0 years (interquartile range 61 to 76). Demographic data and clinical characteristics of the 785 patients are given in Supplementary Table 2a. Study design, inclusion and exclusion criteria have been published previously[19,35]. In brief, patients with atherosclerotic carotid artery disease, as defined by the presence of non-stenotic plaques or atherosclerotic carotid narrowing of any degree, who were neurologically asymptomatic at the time of screening, were enrolled. The indications for performing carotid ultrasound investigation included carotid bruits, cardiovascular risk factors and known atherosclerotic diseases of other vessel areas. Patients with a myocardial infarction (MI), stroke, coronary intervention or peripheral vascular surgery during the preceding 6 months, were excluded from the study. The rationale behind this was the assumption that acute cardiovascular events may affect laboratory measures and reflect the severity of an acute situation rather than chronic atherosclerosis. The study complied with the Declaration of Helsinki and was approved by the review board and the institutional ethics committee of the Medical University of Vienna. All patients gave their written informed consent.

LURIC study. The detailed study design, inclusion and exclusion criteria have been published previously[20]. We analysed 1,514 samples that were randomly selected. Demographic data and clinical characteristics of the 1,514 patients are given in Supplementary Table 3a.

FAST-MI study. The detailed study design, inclusion and exclusion criteria have been published previously[21]. We analysed 974 samples.

Clinical and laboratory data for the ICARAS clinical study

Every patient completed a detailed study questionnaire assessing the patient's medical history, current medication, biometric data, and family history. Physical examination was carried out by a trained physician with special attention to patients' cardiovascular risk factors and comorbidities. All demographic and vital parameters were ascertained by two independent observers. Antecubital venous blood samples were drawn and analysed directly without freezing according to local laboratory standard procedure. In addition, a secondary serum sample from each patient was drawn at baseline visit and directly frozen at −80 °C according to local standard procedures. Colour-coded duplex sonography examinations of carotid arteries at baseline visits were performed on an Acuson128 XP10 with a 7.5-MHZ linear array probe (Acuson, Malvern, PA, USA). Treating physicians and ultrasonographers were blinded for all laboratory values. Definitions of risk factors and comorbidities were published previously[19,35]. Cardiovascular and all-cause mortality were assessed by searching the national death register for the specific cause of death (according to the International Statistical Classification of Diseases and Related Health Problems, 10th Revision). Only the specific cause of death (for example, stroke) was used to categorize death as either all-cause or cardiovascular death. In 43% of deaths, the underlying cause was assessed by autopsy. All demographic and vital parameters were ascertained by two independent observers.

Statistical analyses

Statistical analyses were performed using Graph Pad Prism 8 (Graph Pad Software). Experimental groups were compared using two-tailed Student's unpaired or paired *t*-test or two-tailed Mann–Whitney *U*-test as appropriate. To analyse multiple group data, one-way ANOVA followed by Newman–Keuls or Tukey's test, or two-way ANOVA followed by Sidak's test, were used. Data are presented as mean ± s.e.m. A *P* value of <0.05 was considered significant.

ICARAS clinical study. Serum levels of APRIL or nc-APRIL were categorized in tertiles or quartiles (where indicated) to obtain clinically useful measures of the effect sizes. Continuous data are presented as median and interquartile range (range from the 25th to the 75th percentile). Discrete data are given as counts and percentages. ANOVA (analysis of variance) and the $\chi 2$ test were used for comparisons between tertiles or quartiles, as appropriate. The log-rank test was used for comparison between groups. Event-free survival probabilities were estimated using the Kaplan–Meier method. Univariable and multivariable Cox proportional hazards models were used to assess the association between serum levels of APRIL or nc-APRIL and the occurrence of either all-cause or cardiovascular death, including the following variables: age (years), sex (male/female), history of myocardial infarction (binary), history of stroke (binary), peripheral arterial disease (binary), body mass index (kg/m^2), hypertension (binary), diabetes mellitus (binary), serum creatinine (mg/dl), glycohaemoglobin A1 (%), levels of triglycerides (mg/dl), total cholesterol levels (mg/dl), LDL cholesterol levels (mg/dl), high-sensitivity C-reactive protein (mg/dl), ICAM-1 (ng/ml), VCAM-1 (ng/ml) and statin treatment (binary). The selection of the variables was defined a priori and is based on current guidelines for cardiovascular risk prediction. All of the variables listed above were included in every multivariable Cox proportional hazard model used for this study. The results of the Cox models are presented as hazard ratios (HR; 95% CI). We assessed the overall model fit using Cox–Snell residuals. We also tested the proportional hazard assumption for all covariates using Schoenfeld residuals (overall test) and the scaled Schoenfeld residuals (variable-by-variable testing). A two-sided *P* value of <0.05 was considered significant. All calculations were performed with SPSS (version 20.0, SPSS Inc.) for Windows.

LURIC clinical study. Survival analysis was performed considering the following variables as potential risk factors: serum levels of nc-APRIL, age (years), sex (male/female), body mass index, history of myocardial infarction (no, one, more than one), history of stroke (binary), peripheral arterial disease (binary), body mass index (kg/m^2), hypertension (binary), type II diabetes mellitus (binary), peripheral vascular disease (binary), isolated systolic hypertension (≥140/<90), C-reactive protein (mg/dl) > 0.01 (binary), glycosylated haemoglobin (%), serum creatinine (mg/dl), levels of triglycerides (mg/dl), and total cholesterol levels (mg/dl). Serum levels of nc-APRIL were categorized in quartiles for descriptive purposes and for Kaplan–Meier curves. Baseline characteristics for all variables are provided for the complete dataset and stratified by the nc-APRIL quartiles. Metric variables are presented as mean ± 95% CI. For discrete variables, counts and percentages are given. ANOVA (analysis of variance) and the $\chi 2$ test were used for comparisons between quartiles to provide a quick overview of potential confounding of risk factors with nc-APRIL. Multivariable Cox proportional hazards models were applied to assess the association between the above listed risk factors and the occurrence of either all-cause or cardiovascular death. Owing to very strong right-skewness, the laboratory parameters serum creatinine, triglycerides and cholesterol as well as nc-APRIL were log-transformed. Again, no model selection was performed, and the set of variables was defined a priori based on current guidelines for cardiovascular risk prediction. The results of the Cox models are presented as hazard ratios (HR; 95% CI). The proportional hazard assumption was tested for all covariates using Schoenfeld residuals (overall test) and the scaled Schoenfeld residuals (variable-by-variable testing). A two-sided *P* value of <0.05 was considered significant. All calculations were performed with R version 3.6.0 (https://www.R-project.org/). Survival analysis was performed using the R packages survival

(https://CRAN.R-project.org/package=survival) and survminer (https://CRAN.R-project.org/package=survminer).

FAST-MI clinical study. The primary endpoint was all-cause death during two years of follow-up after the index myocardial infarction. A multivariable Cox proportional-hazards model was used to assess the independent prognostic value of variables with the primary endpoint. The multivariable model comprised age, sex, previous or current smoking, previous myocardial infarction, family history of coronary disease, history of hypertension, diabetes, renal failure, heart rate at admission, heart failure, Killip class, left ventricular ejection fraction, hospital management (including reperfusion therapy, statins, beta blockers, clopidogrel, diuretics, digitalis, heparin), troponin I and log CRP levels.

Reporting summary

Further information on research design is available in the Nature Research Reporting Summary linked to this paper.

Data availability

The RNA sequencing datasets (from vascular smooth muscle cells) are available in the Gene Expression Omnibus with accession codes GSE117963 and GSE17858. All other relevant data are available from the corresponding authors upon reasonable request. Source data are provided with this paper.

Code availability

For the clinical studies, the calculations were performed with SPSS (version 20.0, SPSS Inc.) for Windows, R version 3.6.0 (https://www.R-project.org/), and survival analysis was performed using the R packages survival (https://CRAN.R-project.org/package=survival) and survminer (https://CRAN.R-project.org/package=survminer). For analysis of mass spectrometry data, acquired raw data files were processed using Proteome Discoverer 2.4.1.15 SP1 for DDA experimental data or Skyline version 20.1.0.155 for PRM experimental data or using Mascot version 2.3.02 (Matrix Science, London, UK) and Phenyx (GeneBio, Geneva, Switzerland) as search engines. RNA-seq data were quality controlled using FastQC v0.11.3 (https://www.bioinformatics.babraham.ac.uk/projects/fastqc/) and trimmed using the Trim Galore v0.4.1 wrapper (https://www.bioinformatics.babraham.ac.uk/projects/trim_galore/). Reads were aligned to the GRCm38 mouse reference genome using Tophat v2.0.12. Reads with a minimum map quality of 20 were imported into Seqmonk 1.45.4 (http://www.bioinformatics.babraham.ac.uk/projects/seqmonk).

22. Kowalczyk-Quintas, C. et al. Generation and characterization of function-blocking anti-ectodysplasin A (EDA) monoclonal antibodies that induce ectodermal dysplasia. *J. Biol. Chem.* **289**, 4273–4285 (2014).
23. Chou, M. Y. et al. Oxidation-specific epitopes are dominant targets of innate natural antibodies in mice and humans. *J. Clin. Invest.* **119**, 1335–1349 (2009).
24. Kijani, S., Vázquez, A. M., Levin, M., Borén, J. & Fogelstrand, P. Intimal hyperplasia induced by vascular intervention causes lipoprotein retention and accelerated atherosclerosis. *Physiol. Rep.* **5**, e13334 (2017).
25. Tom, R., Bisson, L. & Durocher, Y. Transfection of HEK293-EBNA1 cells in suspension with linear PEI for production of recombinant proteins. *Cold Spring Harb. Protoc.* https://doi.org/10.1101/pdb.prot4977 (2008).
26. Schindelin, J. et al. Fiji: an open-source platform for biological-image analysis. *Nat. Methods* **9**, 676–682 (2012).
27. Bossen, C. et al. TACI, unlike BAFF-R, is solely activated by oligomeric BAFF and APRIL to support survival of activated B cells and plasmablasts. *Blood* **111**, 1004–1012 (2008).
28. Kowalczyk-Quintas, C. et al. Inhibition of membrane-bound BAFF by the anti-BAFF antibody Belimumab. *Front. Immunol.* **9**, 2698 (2018).
29. Schneider, P., Willen, L. & Smulski, C. R. Tools and techniques to study ligand-receptor interactions and receptor activation by TNF superfamily members. *Methods Enzymol.* **545**, 103–125 (2014).
30. Manza, L. L., Stamer, S. L., Ham, A.-J. L., Codreanu, S. G. & Liebler, D. C. Sample preparation and digestion for proteomic analyses using spin filters. *Proteomics* **5**, 1742–1745 (2005).
31. Wiśniewski, J. R., Zougman, A., Nagaraj, N. & Mann, M. Universal sample preparation method for proteome analysis. *Nat. Methods* **6**, 359–362 (2009).
32. Rappsilber, J., Ishihama, Y. & Mann, M. Stop and go extraction tips for matrix-assisted laser desorption/ionization, nanoelectrospray, and LC/MS sample pretreatment in proteomics. *Anal. Chem.* **75**, 663–670 (2003).
33. Olsen, J. V. et al. Parts per million mass accuracy on an Orbitrap mass spectrometer via lock mass injection into a C-trap. *Mol. Cell. Proteomics* **4**, 2010–2021 (2005).
34. Hellings, W. E., Moll, F. L., de Kleijn, D. P. & Pasterkamp, G. 10-years experience with the Athero-Express study. *Cardiovasc. Diagn. Ther.* **2**, 63–73 (2012).
35. Mayer, F. J. et al. Combined effects of inflammatory status and carotid atherosclerosis: a 12-year follow-up study. *Stroke* **47**, 2952–2958 (2016).
36. Battle, A., Brown, C. D., Engelhardt, B. E. & Montgomery, S. B. Genetic effects on gene expression across human tissues. *Nature* **550**, 204–213 (2017).

Acknowledgements We thank A. Fabry and T. Wenko for help with the in vivo experimental studies, and C. Friedl for help with confocal microscopy. This work was supported by grants from the Austrian Science Fund (SFB F54), the European Union (FP7 VIA) and the Leducq Foundation (TNE-20CVD03) to C.J.B., and by grants from the European Research Area Network on Cardiovascular Diseases (I4647) and the British Heart Foundation (RCAG/917) to D.T. D.T. is also supported by the Austrian Science Fund (I4963). P.S. is supported by the Swiss National Science Foundation (31003A_176256, 310030E_197000). Z.M. is supported by the British Heart Foundation (RCAM/104, RCAM-659, RRCAM.163), the British Heart Foundation Center for Research Excellence (RE/18/1/34212), the NIHR Cambridge Biomedical Research Centre (RG85315), the European Union (FP7 VIA; RCAG/430) and the European Research Council (ERC). T.H. is supported by a NWO Veni grant (91619012).

Author contributions D.T. conceived and designed the study, performed most of the experiments, analysed and interpreted data, and wrote the manuscript. M.E. and P.S. generated materials, performed experiments to characterize nc-APRIL and interpreted data. G.O., L.E., S.K., L.W., T.A., T.H., M.G.K., M.O.-K., L.G., F.P., J.E.M. and P.F. aided in mouse studies and provided technical assistance with the experiments. M.C. aided in immunofluorescence analyses. D.S. aided in mouse studies. J.L. and H.F.J. provided the RNA-seq data for mouse VSMCs. A.M. and J.W. performed the mass-spectrometry analysis and analysed the data. F.J.M. and F.F. performed statistical analysis of the ICARAS and LURIC clinical data, respectively. O.D. and J.B. provided reagents and technical expertise with the experiments, and critically revised the manuscript. M.H. was involved in the analysis of human samples. T.S and N.D. provided the samples from the FAST-MI clinical study and performed the statistical analysis of the data. H.S., W.M. and Z.M. provided the samples from the LURIC clinical study and measured nc-APRIL levels. G.P. provided materials. H.H. provided materials and critically revised the manuscript. Z.M. and P.S. contributed to study design, interpreted data and critically revised the manuscript. C.J.B. designed the study, interpreted data and wrote the manuscript.

Competing interests D.T., C.J.B., P.S. and M.E. are named inventors on a patent application (EP20217536.0; pending) to exploit c-APRIL and nc-APRIL for diagnostic and therapeutic purposes in cardiovascular disease that has been filed by the Medical University of Vienna (Austria) and CeMM Research Center for Molecular Medicine of the Austrian Academy of Sciences (Austria). O.D. is an employee of Adipogen Life Sciences, which provided some reagents used in this study.

Additional information

Supplementary information The online version contains supplementary material available at https://doi.org/10.1038/s41586-021-03818-3.

Correspondence and requests for materials should be addressed to D.T. or C.J.B.

Peer review information *Nature* thanks Peter Libby, William Sessa and the other, anonymous, reviewer(s) for their contribution to the peer review of this work.

a

experimental groups	whole body weight (g)	plasma triglycerides (mg/dL)	en face lesion size (% of total area)
Ldlr$^{-/-}$ *Tnfsf13*$^{+/+}$	22.98 ± 0.74	665.0 ± 53.61	1.89 ± 0.19
Ldlr$^{-/-}$ *Tnfsf13*$^{-/-}$	23.28 ± 0.40	596.9 ± 43.06	1.67 ± 0.20

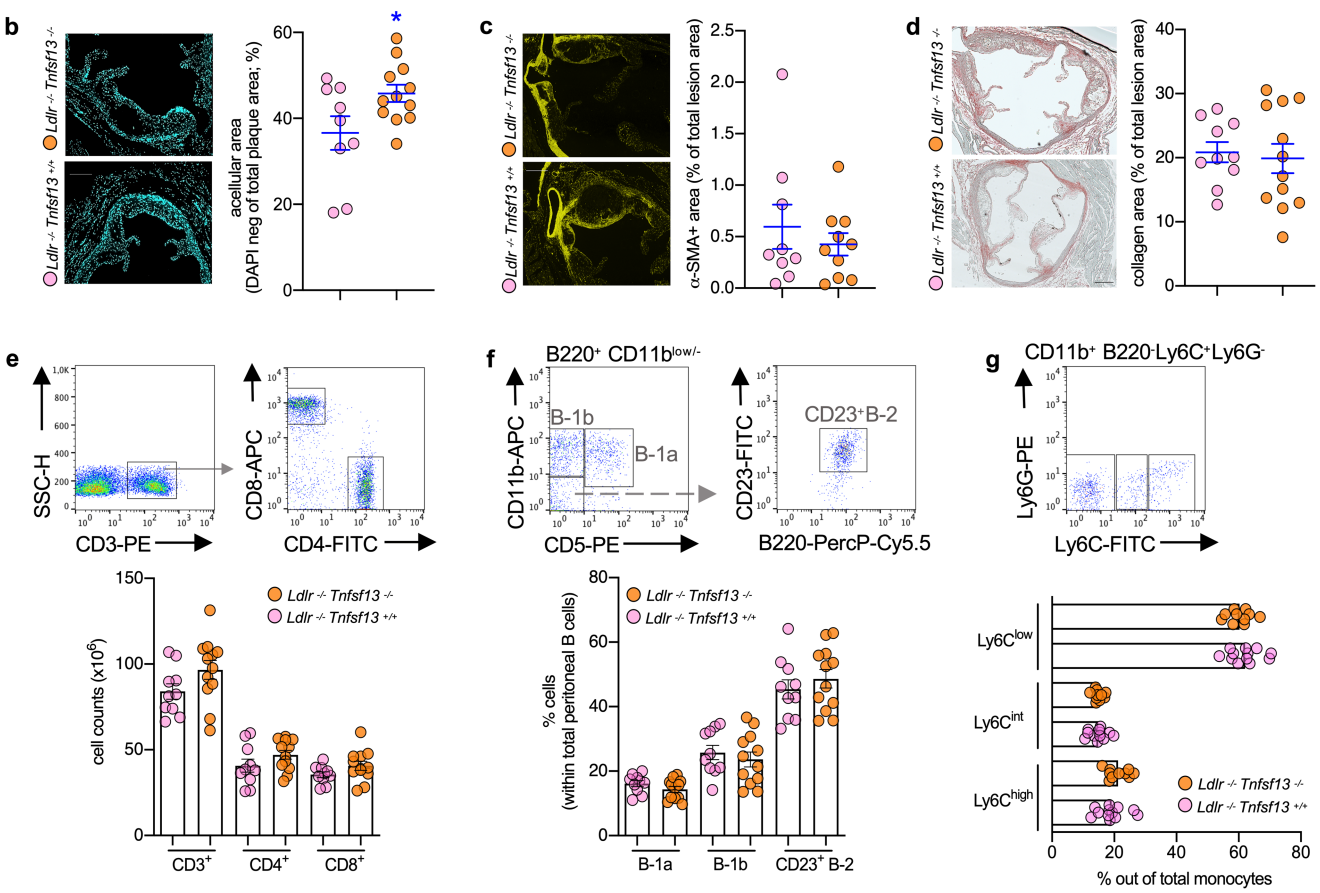

Extended Data Fig. 1 | APRIL deficiency does not alter the plaque smooth muscle cell and collagen content, or the numbers of circulating monocytes, B or T lymphocytes in *Ldlr*$^{-/-}$ mice. *Ldlr*$^{-/-}$*Tnfsf13*$^{+/+}$ or *Ldlr*$^{-/-}$*Tnfsf13*$^{-/-}$ mice were fed an atherogenic diet for 10 weeks. **a**, Whole body weight, plasma triglyceride levels and en face lesion size ($n = 10$ *Ldlr*$^{-/-}$*Tnfsf13*$^{+/+}$ mice, $n = 12$ *Ldlr*$^{-/-}$*Tnfsf13*$^{-/-}$ mice). **b**–**d**, Representative photomicrographs of DAPI- (**b**), α-SMA- (**c**) and Sirius Red-stained lesions (**d**) in the aortic origin (left) and dot plots (right) showing the averaged acellular (**b**; $n = 9$ *Ldlr*$^{-/-}$*Tnfsf13*$^{+/+}$ mice, $n = 12$ *Ldlr*$^{-/-}$*Tnfsf13*$^{-/-}$ mice, $P = 0.036$), α-SMA-positive (**c**, $n = 9$ *Ldlr*$^{-/-}$*Tnfsf13*$^{+/+}$ mice, $n = 10$ *Ldlr*$^{-/-}$*Tnfsf13*$^{-/-}$ mice) and collagen-positive area normalized to total lesion size (**d**; $n = 10$ *Ldlr*$^{-/-}$*Tnfsf13*$^{+/+}$ mice, $n = 12$ *Ldlr*$^{-/-}$*Tnfsf13*$^{-/-}$ mice). **e**–**g**, Representative flow cytometry dot plots (top) and quantification (bottom) of the absolute numbers of splenic CD3$^+$, CD4$^+$ (defined as CD3$^+$CD4$^+$CD8$^-$) and CD8$^+$ T cells (defined as CD3$^+$CD8$^+$CD4$^-$) (**e**), frequencies of peritoneal B-1a (defined as B220^{low}CD11b^{int}CD5$^+$), B-1b (defined as B220^{low}CD11b^{int}CD5$^-$) and CD23$^+$ B-2 (defined as B220^{high}CD11b$^-$CD5$^-$CD23$^+$) cells (**f**) and the frequencies of circulating Ly6C^{high}, Ly6C^{int} and Ly6C^{low} monocytes (**g**) in peripheral blood. All results show mean (two-tailed unpaired Student's *t*-test). Scale bars, 200 µm.

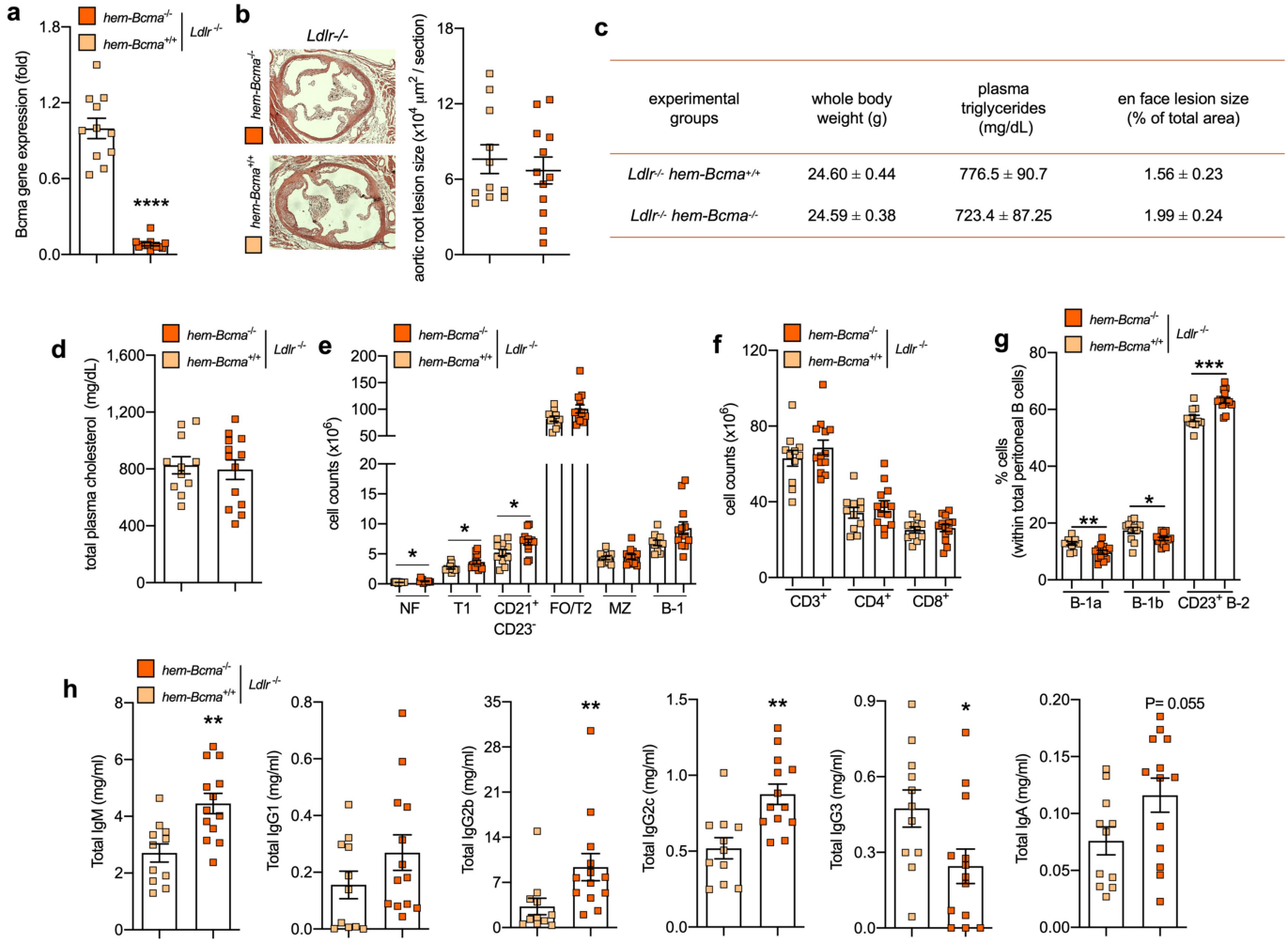

experimental groups	whole body weight (g)	plasma triglycerides (mg/dL)	en face lesion size (% of total area)
Ldlr$^{-/-}$ hem-*Bcma*$^{+/+}$	24.60 ± 0.44	776.5 ± 90.7	1.56 ± 0.23
Ldlr$^{-/-}$ hem-*Bcma*$^{-/-}$	24.59 ± 0.38	723.4 ± 87.25	1.99 ± 0.24

Extended Data Fig. 2 | BCMA is dispensable for atherosclerosis development. Lethally irradiated *Ldlr*$^{-/-}$ mice were injected with bone marrow from *Bcma*$^{+/+}$ (hem-*Bcma*$^{+/+}$) or *Bcma*$^{-/-}$ donors (hem-*Bcma*$^{-/-}$) and were fed an atherogenic diet for 10 weeks. **a**, *Bcma* mRNA in the spleen ($n = 11$ hem-*Bcma*$^{+/+}$, $n = 13$ hem-*Bcma*$^{-/-}$ mice). **b**, Representative photomicrographs of H&E-stained aortic root lesions (left) and average lesion size in the aortic origin (right) expressed as µm^2 per section ($n = 11$ hem-*Bcma*$^{+/+}$, $n = 12$ hem-*Bcma*$^{-/-}$ mice). **c**, Whole body weight, plasma triglyceride levels and en face lesion size ($n = 11$ hem-*Bcma*$^{+/+}$, $n = 13$ hem-*Bcma*$^{-/-}$ mice). **d**, Total plasma cholesterol ($n = 11$ hem-*Bcma*$^{+/+}$, $n = 13$ hem-*Bcma*$^{-/-}$ mice). **e**, Absolute numbers of FO/T2, MZ, CD21$^+$CD23$^-$ ($P = 0.028$), T1 ($P = 0.023$), NF ($P = 0.031$) and B-1 B cells ($n = 11$ hem-*Bcma*$^{+/+}$, $n = 13$ hem-*Bcma*$^{-/-}$ mice). **f**, Absolute numbers of CD3$^+$, CD4$^+$ and CD8$^+$ T cells ($n = 11$ hem-*Bcma*$^{+/+}$, $n = 13$ hem-*Bcma*$^{-/-}$ mice). **g**, **h**, Frequencies of peritoneal B-1a ($P = 0.003$), B-1b ($P = 0.021$) and CD23$^+$ B-2 cells ($P = 0.0003$) (**g**) and total IgM ($P = 0.002$), IgG1, IgG2b ($P = 0.002$), IgG2c ($P = 0.001$), IgG3 ($P = 0.032$) and IgA plasma antibody titers (**h**; $n = 11$ hem-*Bcma*$^{+/+}$, $n = 13$ hem-*Bcma*$^{-/-}$ mice). All results show mean ± s.e.m. *$P < 0.05$, **$P < 0.01$, ***$P < 0.001$, ****$P < 0.0001$ (two-tailed Mann–Whitney *U*-test or two-tailed unpaired Student's *t*-test). Scale bar, 200 µm.

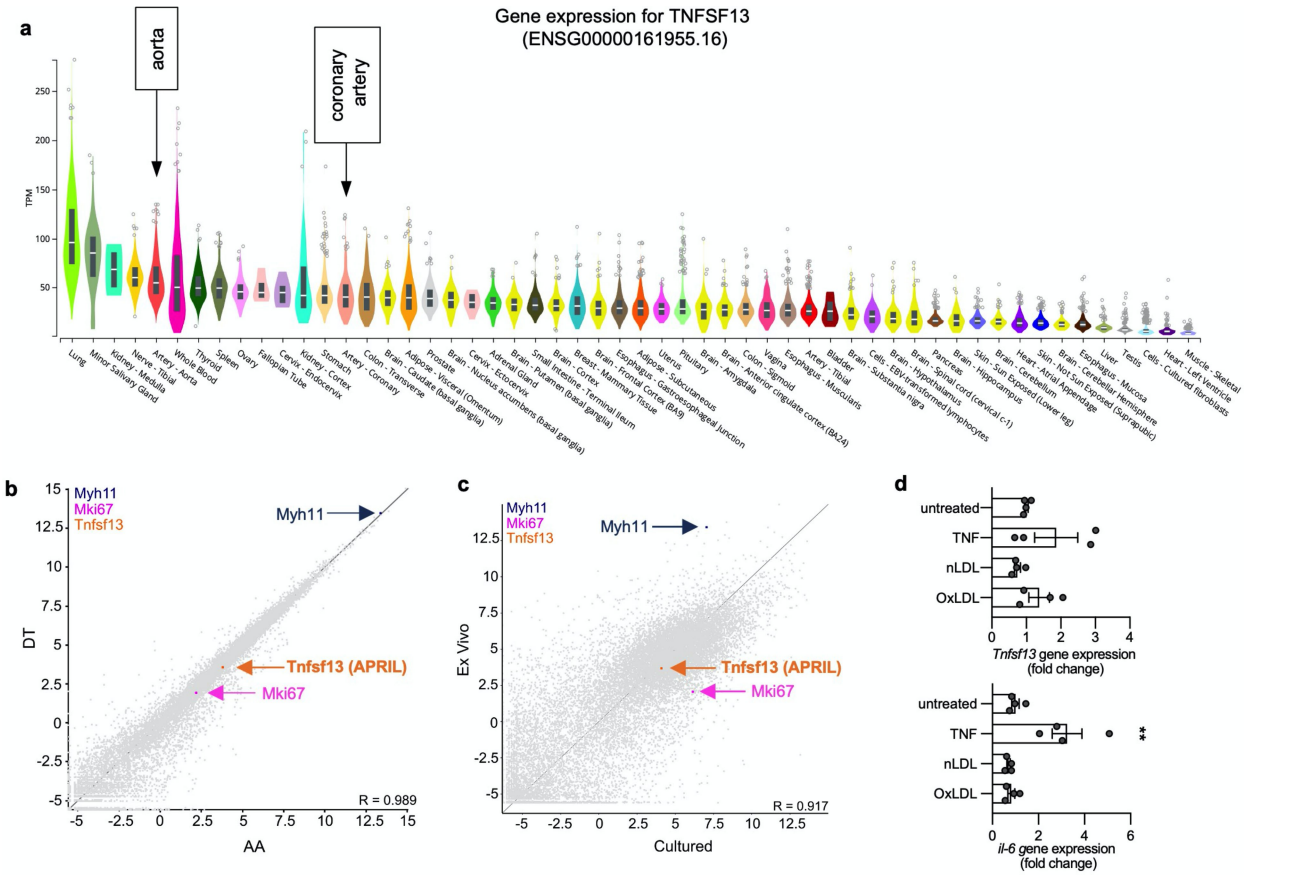

Extended Data Fig. 3 | APRIL is produced by mouse and human VSMCs. **a**, *TNFSF13* gene expression in human tissues in the Genotype-Tissue Expression (GTEx) project[36]. The GTEx project was supported by the Common Fund of the Office of the Director of the National Institutes of Health, and by NCI, NHGRI, NHLBI, NIDA, NIMH, and NINDS. The data described in this manuscript were obtained from the GTEx Portal on 21 January 2021 and dbGaP accession number phs000424.v8.p2. The results show median (aorta: median = 55.05, $n = 432$; coronary artery: median = 40.7, $n = 240$). **b**, **c**, Bulk RNA-seq analysis of VSMCs from the aortic arch (AA) and descending thoracic aorta (DT) (**b**; $n = 3–5$ mice) (GSE117963) and from mouse primary VSMCs that were stored in Trizol after isolation or had been cultured for 4–5 passages until the analysis (**c**; GSE17858). *TNFSF13*, *MYH11* and *KI67* gene expression are depicted. **d**, *TNFSF13* and *IL6* gene expression by human umbilical artery smooth muscle cells that were stimulated in quadruplicate with recombinant human TNF, native human LDL or human oxLDL (TNF stimulation is representative of three independent experiments; $P = 0.003$). Results show mean ± s.e.m. $^{**}P < 0.01$ (one-way ANOVA and Tukey's test).

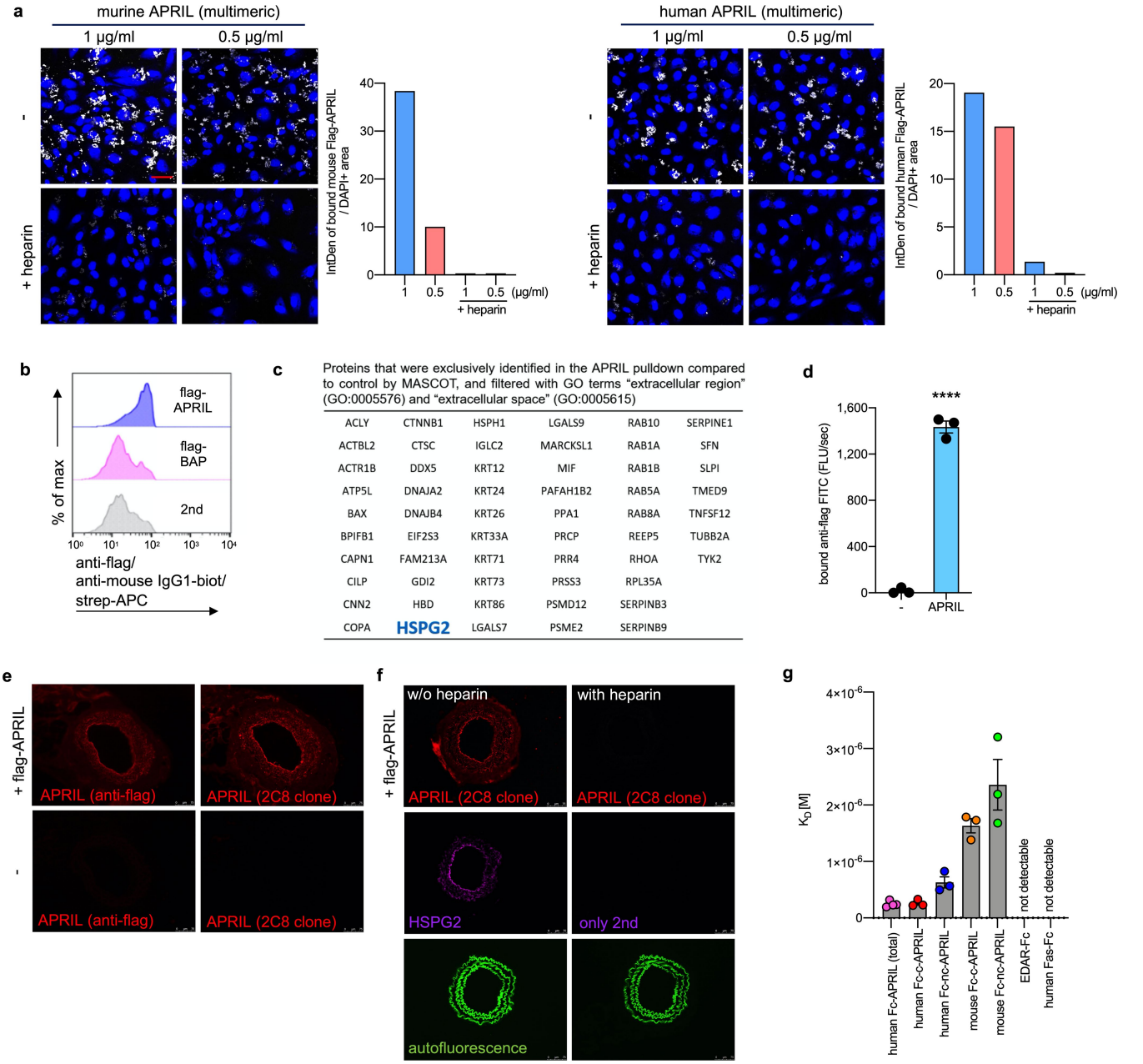

Extended Data Fig. 4 | APRIL binds HSPG2. a, Representative photomicrographs (left) and quantification (right) of HUVECs incubated with either human or mouse Flag–APRIL in the presence or absence of heparin and stained with the anti-Flag M2 antibody conjugated to FITC and analysed by confocal microscopy. **b**, Flow cytometry analysis of HUVECs incubated with Flag–APRIL or flag-tagged bacterial alkaline phosphatase (Flag–BAP) and stained with the anti-Flag M2 antibody. **c**, Identification of protein binding partners of APRIL in HUVEC culture by performing a pull-down assay with agarose beads coupled to the anti-Flag M2 antibody followed by MS analysis. **d**, APRIL binding to coated HSPGs from mouse basement membrane quantified by ELISA determined in triplicate (****$P < 0.0001$, two-tailed unpaired Student t test). Data shown are representative of at least two independent experiments (**a**, **b**, **d**). **e**, **f**, Photomicrographs of mouse carotid artery sections incubated with mouse multimeric Flag–APRIL and stained with either an anti-Flag antibody conjugated to PE or with an anti-mouse APRIL biotinylated antibody (2C8) and streptavidin conjugated to PE (**e**; scale bar, 75 µm, data derived from two independent experiments) or with mouse multimeric Flag–APRIL in the presence or absence of heparin and stained with an anti-APRIL biotinylated antibody (2C8) or with an anti-HSPG2 or only secondary antibody (only 2nd) (**f**; scale bar, 75 µm, data derived from one experiment). **g**, Quantitative surface plasmon resonance (Biacore) analysis of the affinity of soluble human Fc–APRIL (total), human canonical Fc–APRIL (human Fc–c-APRIL), human non-canonical Fc–APRIL (human Fc–nc-APRIL), mouse canonical Fc–APRIL (mouse Fc–c-APRIL), mouse non-canonical Fc–APRIL (mouse Fc–nc-APRIL) and negative controls EDAR–Fc and human Fas–Fc to biotinylated heparin coupled to streptavidin Sensor Chip A ($n = 3$ independent experiments). All results show mean ± s.e.m. IntDen, integrated density.

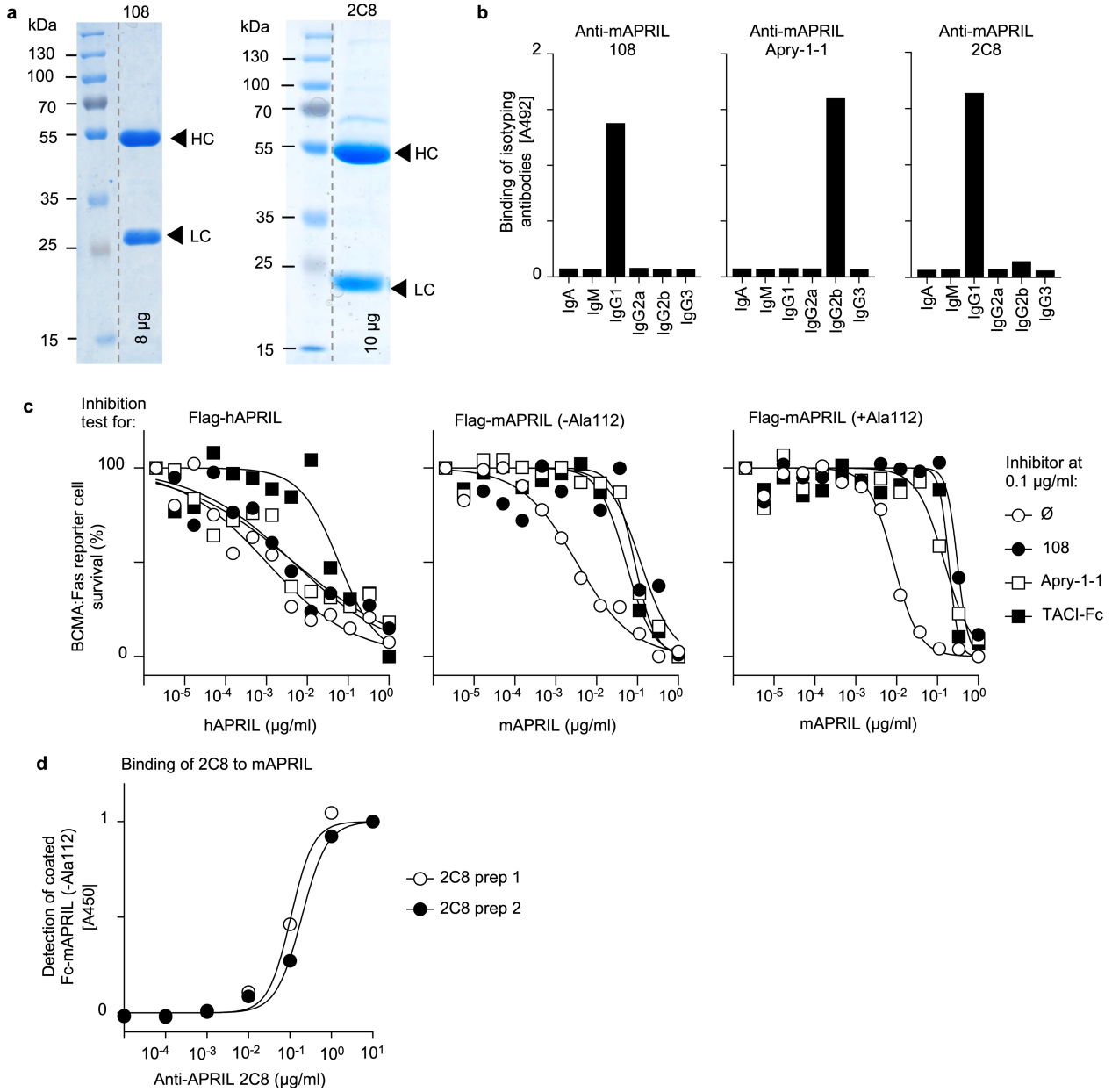

Extended Data Fig. 5 | Anti-APRIL antibodies 108, 2C8 and Apry-1-1 are specific for mouse APRIL. a, Coomassie blue analyses of anti-mAPRIL mAb 108 and 2C8 under reducing conditions. **b**, Isotyping of the Fc portions of anti-mAPRIL 108, Apry-1-1 and 2C8. Purified antibodies coated on an ELISA plate were revealed with peroxidase-conjugated antibodies against different isotypes. **c**, Inhibitory activity of 108 and Apry-1-1 compared to that of TACI-Fc on human and mouse APRIL. Flag–human APRIL and two splice variants of Flag–mouse APRIL (±Ala112) were titrated on BCMA–Fas reporter cells in the presence of a fixed, non-saturating concentration of 108, Apry-1-1 or TACI-Fc. The data show that 108 and Apry-1-1 inhibit both splice variants of mAPRIL at roughly stoichiometric ratios, but do not cross-react with human APRIL. **d**, ELISA for 2C8 binding to mouse APRIL. Binding of 2C8 to plates coated with human Fc–mouse APRIL was evaluated with a peroxidase-coupled anti-mouse antibody. **a**, **b**, Data are representative of two independent experiments.

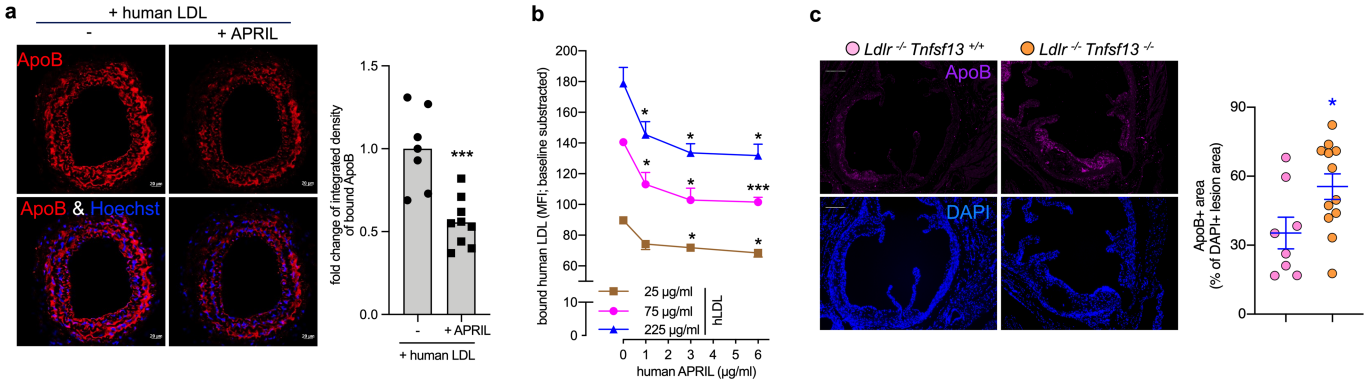

Extended Data Fig. 6 | APRIL competes for binding of LDL to proteoglycans. **a**, Representative photomicrographs (left) and quantification (right) of anti-ApoB antibody binding to mouse carotid artery sections incubated with human native LDL in the presence or absence of mouse multimeric Flag–APRIL analysed by both confocal and epifluorescence microscopy (without APRIL, $n = 7$; with APRIL, $n = 9$; $P = 0.0004$). **b**, The amount of bound human LDL (triplicate; quantified by flow cytometry) on the surface of HEK293 wild-type cells in the presence of different amounts of human recombinant APRIL. **c**, Representative photomicrographs of ApoB-stained lesions in the aortic origin (left) and ApoB-positive area normalized to DAPI$^+$ lesion area (right) of *Ldlr*$^{-/-}$*Tnfsf13*$^{+/+}$ or *Ldlr*$^{-/-}$*Tnfsf13*$^{-/-}$ mice that were fed an atherogenic diet for 10 weeks ($n = 8$ *Ldlr*$^{-/-}$*Tnfsf13*$^{+/+}$ mice, $n = 12$ *Ldlr*$^{-/-}$*Tnfsf13*$^{-/-}$ mice; $P = 0.035$). Data shown are pooled from four independent experiments with seven to nine sections per group (**a**), representative of three independent experiments (**b**). All results show mean ± s.e.m. $^*P < 0.05$, $^{***}P < 0.001$ (two-tailed unpaired Student's *t*-test). Scale bars, 20 µm (**a**) and 200 µm (**c**).

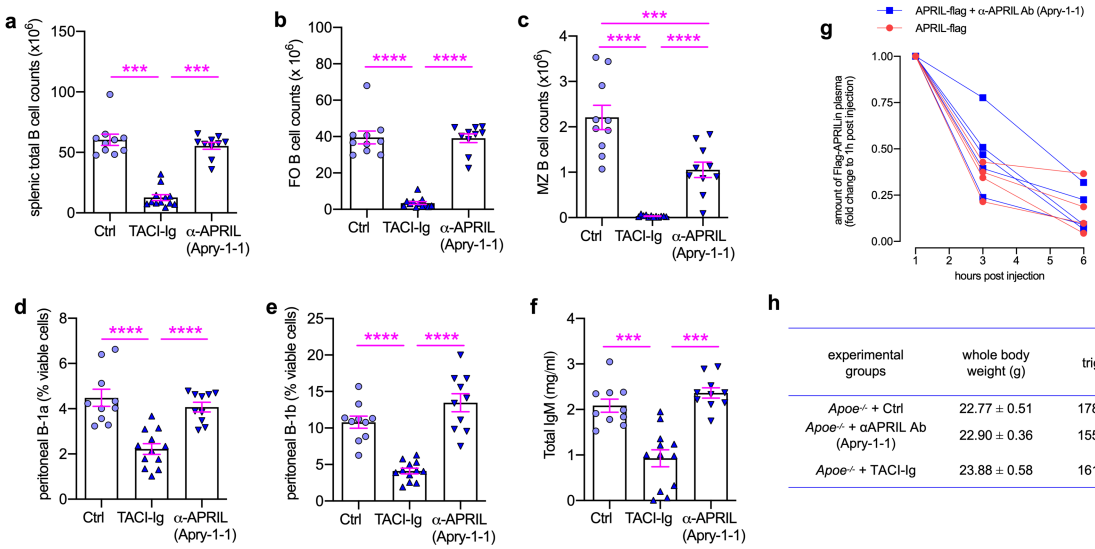

h

experimental groups	whole body weight (g)	plasma triglycerides (mg/dL)	plasma cholesterol (mg/dL)
Apoe$^{-/-}$ + Ctrl	22.77 ± 0.51	178.8 ± 14.80	1606 ± 83
Apoe$^{-/-}$ + αAPRIL Ab (Apry-1-1)	22.90 ± 0.36	155.0 ± 15.16	1513 ± 86
Apoe$^{-/-}$ + TACI-Ig	23.88 ± 0.58	161.5 ± 12.92	1645 ± 62

Extended Data Fig. 7 | Treatment with the blocking anti-APRIL antibody Apry1-1 does not alter B cells, IgM and plasma lipid levels in *Apoe*$^{-/-}$ mice. *Apoe*$^{-/-}$ mice were treated biweekly for 10 weeks with a mixture of anti- mouse APRIL antibody (Apry-1-1) and control-Ig (anti-APRIL group), or TACI-Ig and isotype IgG2b (TACI-Ig group), or isotype IgG2b and control-Ig (control group) and were fed an atherogenic diet for the last 8 weeks of the study. **a**–**f**, Dot plots show the numbers of total splenic B cells (**a**), follicular (FO) B cells (**b**), marginal zone (MZ) B cells (**c**), and frequencies of peritoneal B-1a (**d**), peritoneal B-1b (**e**) and total IgM antibody levels (**f**) in plasma. **g**, Wild-type mice were injected intraperitoneally with either 1 µg mouse multimeric Flag–APRIL or a mixture of 1 µg Flag–APRIL and 10 µg anti-mouse APRIL antibody (Apry-1-1). The amount of Flag–APRIL in plasma was measured by ELISA one, three and six hours after the injection ($n = 4$ mice Flag–APRIL, $n = 5$ mice Flag–APRIL + anti-APRIL (Apry1-1)). **h**, Whole body weight, plasma triglyceride and cholesterol levels. **a**–**f**, **h**, All results show mean ± s.e.m.; ($n = 10$ *Apoe*$^{-/-}$ control, $n = 12$ *Apoe*$^{-/-}$ TACI-Ig, $n = 10$ *Apoe*$^{-/-}$ anti-APRIL). ***$P < 0.001$, ****$P < 0.0001$ (one-way ANOVA and Newman–Keuls test).

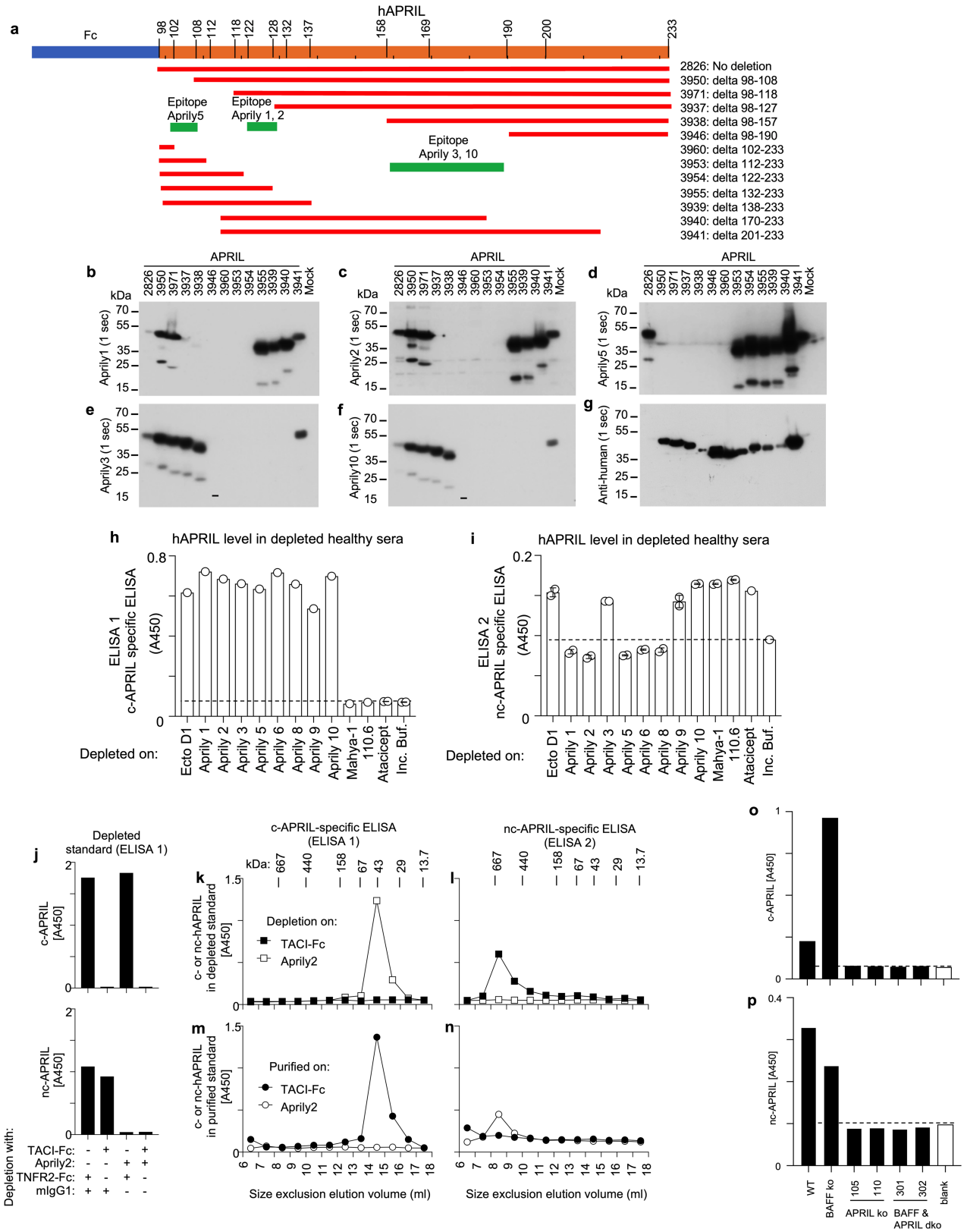

Extended Data Fig. 8 | See next page for caption.

Extended Data Fig. 8 | Epitope mapping of anti-human APRIL antibodies, and native canonical and non-canonical APRIL differ in size but are produced by the same gene. a–**g**, Epitope mapping of anti-human APRIL antibodies. **a**, The epitopes recognized by Aprily1, 2, 3, 5 and 10 were mapped by western blot of truncated APRIL proteins. **b**–**d**, Aprily5 and Aprily1 or Aprily2 recognize distinct epitopes (**d**), whereas Aprily3 and Aprily10 recognize epitopes distinct from those of Aprily1, Aprily2 and Aprily5 (**e**, **f**). **g**, Expression of all constructs was validated by western blot with anti-Fc antibody. **h**, **i**, Human serum was depleted of APRIL using the anti-human APRIL antibodies Aprily1, Aprily2, Aprily3, Aprily5, Aprily6, Aprily8, Aprily9, Aprily10, Mahya-1, 110.6, the biological atacicept (TACI-Ig: a recombinant fusion protein of the receptor TACI and the Fc region of Ig, that binds to APRIL) or the negative control EctoD1, and then analysed with a c-APRIL-specific (**h**; ELISA 1) or an nc-APRIL-specific ELISA (**i**; ELISA 2). Data are derived from one experiment in this format. **j**–**n**, Native canonical and non-canonical APRIL differ in size. **j**, Flag–human APRIL (from c-APRIL ELISA 1 standards) was depleted on TACI–Fc (or TNFR2–Fc as control) and/or on Aprily2 (or mIgG1 as control). APRIL was then detected by c-APRIL-specific (top) or nc-APRIL-specific (bottom) ELISA. **k**, **l**, Flag–human APRIL (from APRIL ELISA 1 standards) was depleted on immobilized TACI–Fc or on Aprily2, and the flow-through was then size-fractionated by size exclusion chromatography (SEC) and detected in fractions by c-APRIL-specific (**k**; ELISA 1) or nc-APRIL-specific (**l**; ELISA 2) ELISA. TACI–Fc and Aprily2 beads used for depletion were then acid-eluted. **m**, **n**, The neutralized eluate was size-fractionated, and APRIL in fractions was detected with c-APRIL-specific (**m**) or nc-APRIL-specific (**n**) ELISA. These results indicate that Flag–c-APRIL has the size of a 3-mer, whereas nc-APRIL is much larger. **o**, **p**, Canonical and non-canonical APRIL are produced by the same *TNFSF13* gene locus. The *TNFSF13* gene (which encodes APRIL) was inactivated in human macrophage cell line U937 by CRISPR–Cas9 technology. As a control, the *TNFSF13B* gene (which encodes BAFF) was also deleted. APRIL in supernatants was measured with a c-APRIL-specific (**o**) and an nc-APRIL-specific (**p**) ELISA. 105, 110, 301 and 302 depict different clones.

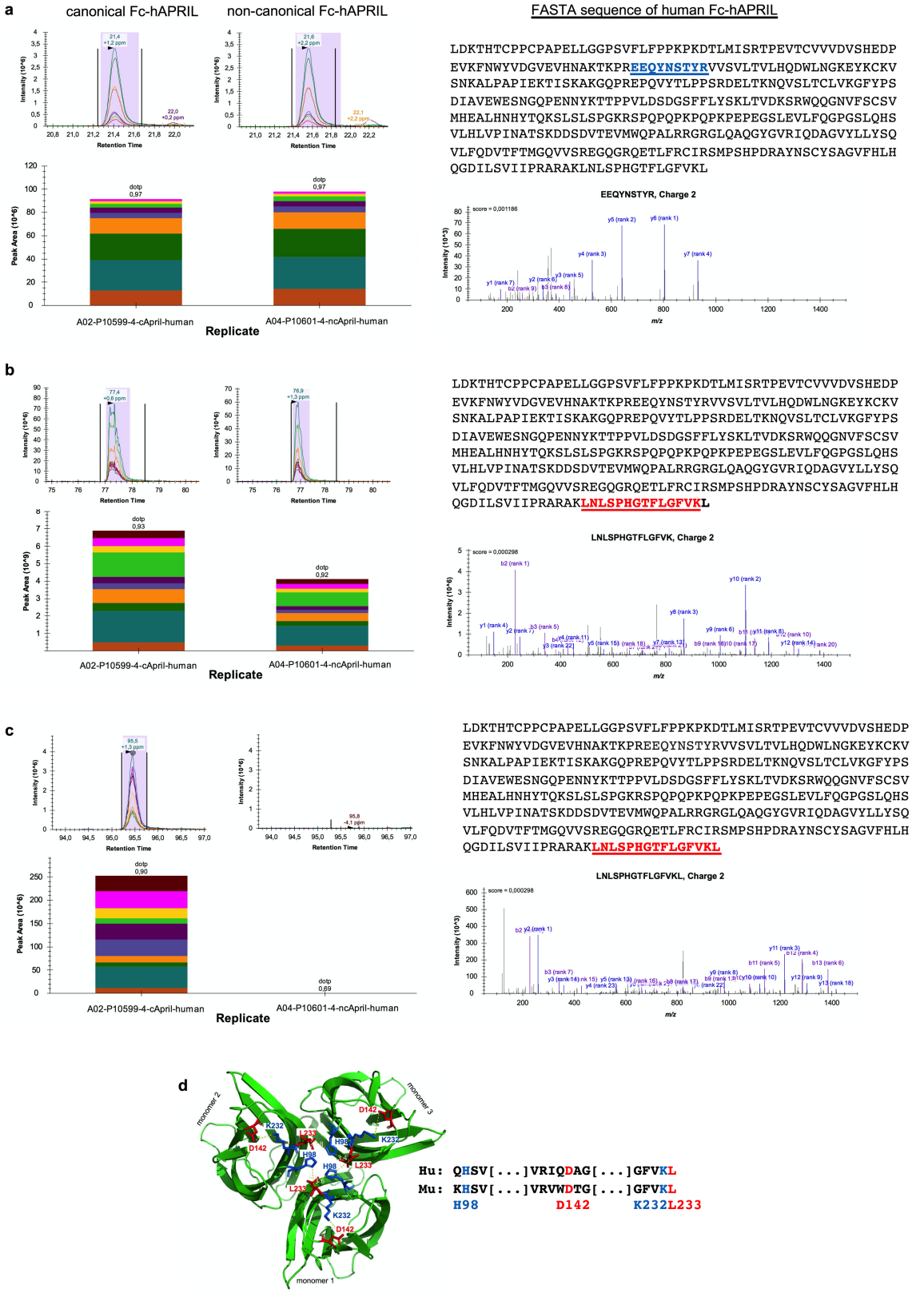

Extended Data Fig. 9 | See next page for caption.

Extended Data Fig. 9 | LC–MS-based parallel reaction monitoring (PRM) analysis of tryptic digest of purified human canonical or non-canonical Fc–APRIL. a–**c**, Raw data were analysed using Skyline software and extracted product ion chromatograms (XICs) are shown either in the form of peaks (top) or total sum of integrated product ion areas (bottom) for the three selected peptides EEQYNSTYR (Fc part) (**a**), LNLSPHGTFLGFVK (tryptic C terminus APRIL) (**b**) and LNLSPHGTFLGFVKL (miscleaved tryptic C terminus APRIL) (**c**). MS2 fragment ion spectra for the selected peptide precursor ions are illustrated at bottom right. Although the peptide shown in **a** is representative for comparable injection amounts of canonical versus non-canonical Fc–APRIL, the C-terminal miscleaved full tryptic peptide shown in **c** is undetectable in non-canonical APRIL. Relative abundances are given in arbitrary units. Right, FASTA sequence of Fc–APRIL with selected tryptic peptide sequences highlighted in blue or red. Note the different scales in **b** (10^9) and **c** (10^6). **d**, Structure of human c-APRIL highlighting the importance of the C terminus for the folding of the different forms (canonical and non-canonical) of APRIL. The representation based on protein data bank accession number 1XU1 highlights the last two C-terminal amino acids (Lys232, Leu233). The N-terminal amino acid of the TNF homology domain (His98) and Asp142 are also shown. All of these residues are conserved in mouse APRIL and human APRIL, although the sequence surrounding Asp142 is different in mouse and human. The C-terminal carboxylic group of Leu233 is very close to His98 of the same monomer (3.6 Å, 4.1 Å and 3.4 Å in the three monomers) and also very close to His98 of the neighbouring monomer (4.3 Å, 3.8 Å and 3.8 Å). Thus, His98 and the carboxylic group or Leu233 seem to form a ring of six salt bridges at the top surface of APRIL. In addition, Lys232 contacts Asp142 (4.3 Å, 4.3 Å and 5.7 Å in the three mouse APRIL monomers), and is only 3.2 Å from Asp142 in human APRIL (PDB accession number 4ZCH).

Extended Data Table 1 | Human clinical studies

a

ICARAS (nc-APRIL)

Variable	Univariate			Multivariate		
	Hazard ratio	CI	P-value	Hazard ratio	CI	P-value
All-cause mortality						
3rd Tertile* (>6.47 ng/ml)	-	-	-	-	-	-
2nd Tertile (4.23-6.47 ng/ml)	1.17	0.90-1.52	0.25	1.31	0.97-1.77	0.07
1st Tertile (<4.22 ng/ml)	1.99	1.56-2.54	<0.01	1.95	1.48-2.56	<0.01
Cardiovascular mortality						
3rd Tertile* (>6.47 ng/ml)	-	-	-	-	-	-
2nd Tertile (4.23-6.47 ng/ml)	1.08	0.76-1.52	0.68	1.28	0.86-1.91	0.22
1st Tertile (<4.22 ng/ml)	2.27	1.67-3.07	<0.01	2.20	1.56-3.12	<0.01

*Reference Category

b

ICARAS (c-APRIL)

Variable	Univariate		Multivariate	
	Hazard ratio	P-value	Hazard ratio	P-value
All-cause mortality				
3rd Tertile* (>2.54 ng/ml)	-	-	-	-
2nd Tertile (1.67-2.54 ng/ml)	1.03	0.82	0.94	0.67
1st Tertile (<1.67 ng/ml)	1.07	0.63	1.13	0.41
Cardiovascular mortality				
3rd Tertile* (>2.54 ng/ml)	-	-	-	-
2nd Tertile (1.67-2.54 ng/ml)	0.89	0.38	0.78	0.21
1st Tertile (<1.67 ng/ml)	1.0	0.89	1.19	0.35

*Reference Category

c

LURIC (nc-APRIL)

Parameter	Hazard ratio	Lower .95	Upper .95	P values
Log nc-APRIL	1.14	1.02	1.27	0.022
age	1.06	1.04	1.07	<0.001
sex	0.70	0.53	0.92	0.011
CRP	1.38	0.95	2.01	0.087
Triglycerides (log)	0.84	0.63	1.12	0.230
Total cholesterol (log)	1.26	0.86	1.85	0.240
Myocardial infarction (no vs one)	1.06	0.82	1.37	0.666
Myocardial infarction (no vs >one)	1.93	1.33	2.81	0.001
Stroke	1.61	1.17	2.22	0.003
Periph. Vasc. Disease	1.83	1.33	2.50	<0.001
BMI	0.98	0.95	1.02	0.331
Isolated systolic hypertension (>=140/<90)	0.83	0.65	1.06	0.140
Type II diabetes	1.25	0.89	1.76	0.189
Creatinine (log)	1.86	1.19	2.90	0.007
Hba1c (%)	1.25	1.13	1.39	<0.001

d

FAST-MI (nc-APRIL)

Variable	Multivariate		
	Hazard ratio	CI	P-value
All-cause death			
3rd Tertile	1.91	1.25-2.91	0.0006
2nd Tertile	0.77	0.45-1.33	ns
1st Tertile *	-	-	-

*Reference Category

a, Univariate and multivariate Cox regression analyses of the ICARAS study (nc-APRIL). First tertile includes patients with nc-APRIL levels lower than 4.22 ng ml^{-1}, second tertile patients with nc-APRIL levels between 4.23 and 6.47 ng ml^{-1}, and the third tertile patients with nc-APRIL levels above 6.47 ng ml^{-1}. Adjusted for age, sex, body mass index, smoking, hypertension, LDL cholesterol levels, triglyceride levels, statin treatment, glycohaemoglobin A1 level, diabetes mellitus, history of myocardial infarction, history of peripheral artery disease, history of stroke, and serum creatinine, intercellular adhesion molecule-1, vascular cell adhesion molecule-1, and high-sensitivity C-reactive protein. The third tertile serves as the reference category (n = 785). **b**, Univariate and multivariate Cox regression analyses of the ICARAS study (c-APRIL). First tertile includes patients with APRIL levels lower than 1.67 ng ml^{-1}, second tertile patients with APRIL levels between 1.67 and 2.54 ng ml^{-1}, and the third tertile patients with APRIL levels above 2.54 ng ml^{-1}. Adjusted for age, sex, body mass index, smoking, hypertension, LDL cholesterol levels, triglyceride levels, statin treatment, glycohaemoglobin A1 level, diabetes mellitus, history of myocardial infarction, history of peripheral artery disease, history of stroke, and serum creatinine, intercellular adhesion molecule-1, vascular cell adhesion molecule-1, and high-sensitivity C-reactive protein. The third tertile serves as the reference category (n = 730). **c**, Multivariate Cox regression analyses for cardiovascular mortality in the LURIC study (nc-APRIL). Adjusted for age (years), sex (male/female), C-reactive protein (mg dl^{-1}), triglycerides (mg dl^{-1}), total cholesterol levels (mg dl^{-1}), history of myocardial infarction (binary), history of stroke (binary), peripheral arterial disease (binary), body mass index (kg/m^2), hypertension (binary), diabetes mellitus (binary), serum creatinine (mg dl^{-1}), haemoglobin 1AC (per cent) (n = 1,514). **d**, Multivariate Cox regression analyses for the FAST-MI study. Circulating levels of nc-APRIL in patients at admission for acute myocardial infarction are associated with cardiovascular outcomes at follow-up. The probability of death during 2 years of follow-up as a function of baseline circulating plasma nc-APRIL levels (n = 974). Results are expressed as hazard ratios (HR) with 95% CI.

nature research

Corresponding author(s): Dr. Dimitrios Tsiantoulas
Dr. Christoph Binder

Last updated by author(s): Jun 24, 2021

Reporting Summary

Nature Research wishes to improve the reproducibility of the work that we publish. This form provides structure for consistency and transparency in reporting. For further information on Nature Research policies, see Authors & Referees and the Editorial Policy Checklist.

Statistics

For all statistical analyses, confirm that the following items are present in the figure legend, table legend, main text, or Methods section.

n/a	Confirmed
☐	☒ The exact sample size (*n*) for each experimental group/condition, given as a discrete number and unit of measurement
☐	☒ A statement on whether measurements were taken from distinct samples or whether the same sample was measured repeatedly
☐	☒ The statistical test(s) used AND whether they are one- or two-sided *Only common tests should be described solely by name; describe more complex techniques in the Methods section.*
☐	☒ A description of all covariates tested
☐	☒ A description of any assumptions or corrections, such as tests of normality and adjustment for multiple comparisons
☐	☒ A full description of the statistical parameters including central tendency (e.g. means) or other basic estimates (e.g. regression coefficient) AND variation (e.g. standard deviation) or associated estimates of uncertainty (e.g. confidence intervals)
☒	☐ For null hypothesis testing, the test statistic (e.g. *F*, *t*, *r*) with confidence intervals, effect sizes, degrees of freedom and *P* value noted *Give P values as exact values whenever suitable.*
☒	☐ For Bayesian analysis, information on the choice of priors and Markov chain Monte Carlo settings
☒	☐ For hierarchical and complex designs, identification of the appropriate level for tests and full reporting of outcomes
☐	☒ Estimates of effect sizes (e.g. Cohen's *d*, Pearson's *r*), indicating how they were calculated

Our web collection on statistics for biologists contains articles on many of the points above.

Software and code

Policy information about availability of computer code

Data collection	BD CellQuest Pro, BD FACS Accuri C6 and LSRFortessa-FACS Diva (BD) softwares were used to collect flow cytometry data. Zeiss Zen software was used to collect microscopy data.
Data analysis	Flow cytometric analyses were performed with FlowJo software (FlowJo 7.6.5). Fiji software was used to analyze image data. Graph Pad Prism 8 was used for the statistical analyses of the experimental studies. For the clinical studies, the calculations were performed with SPSS (version 20.0, SPSS Inc) for Windows, R version 3.6.0 (https://www.R-project.org/), survival analysis was performed using the R packages survival (https://CRAN.R-project.org/package=survival) and survminer (https://CRAN.R-project.org/package=survminer). For analysis of mass-spectometry data, acquired raw data files were processed using Proteome Discoverer 2.4.1.15 SP1 for DDA experimental data or Skyline version 20.1.0.155 for PRM experimental data or using Mascot version 2.3.02 (Matrix Science, London, UK) and Phenyx (GeneBio, Geneva, Switzerland) as search engines. RNA-Seq data were quality controlled using FastQC v0.11.3 (https://www.bioinformatics.babraham.ac.uk/projects/fastqc/) and trimmed using the Trim Galore v0.4.1 wrapper (https://www.bioinformatics.babraham.ac.uk/projects/trim_galore/). Reads were aligned to the GRCm38 mouse reference genome using Tophat v2.0.12 (Trapnell et al 2009). Reads with a minimum map quality of 20 were imported into Seqmonk 1.45.4 (http://www.bioinformatics.babraham.ac.uk/projects/seqmonk).

For manuscripts utilizing custom algorithms or software that are central to the research but not yet described in published literature, software must be made available to editors/reviewers. We strongly encourage code deposition in a community repository (e.g. GitHub). See the Nature Research guidelines for submitting code & software for further information.

Data

Policy information about availability of data

All manuscripts must include a data availability statement. This statement should provide the following information, where applicable:

- Accession codes, unique identifiers, or web links for publicly available datasets
- A list of figures that have associated raw data
- A description of any restrictions on data availability

The RNA sequencing datasets (from vascular smooth muscle cells) are available in the Gene Expression Omnibus with accession codes GSE117963 and GSE17858. All other relevant data are available from the corresponding authors upon reasonable request. Source data of Figures 1, 2, 3, 4 and Extended Data figures 1, 2, 5, 6, 7 and 8 are included within the paper. Supplemental Information is available for this paper.

Field-specific reporting

Please select the one below that is the best fit for your research. If you are not sure, read the appropriate sections before making your selection.

☒ Life sciences ☐ Behavioural & social sciences ☐ Ecological, evolutionary & environmental sciences

For a reference copy of the document with all sections, see nature.com/documents/nr-reporting-summary-flat.pdf

Life sciences study design

All studies must disclose on these points even when the disclosure is negative.

Sample size	For experimental atherosclerosis studies power calculations were performed to determine sample size using data from previous experiments in our lab, and are included in the approved study plan by the Animal Ethics Committee of the Medical University of Vienna.
Data exclusions	One mouse was excluded due to low plasma cholesterol despite atherogenic diet feeding and two other mice (in different studies) as mathematic outliers (abnormally big plaque size in the aortic root and thoracic aorta); the mathematical criteria for the latter was: > mean +2.3xSD, which were defined a priori.
Replication	All attempts at replication were successful. Where appropriate pooled data of all independent experiments are shown.
Randomization	Where appropriate, the mice were selected at random. Otherwise, animals from different experimental groups of each study were co-housed (in a similar ratio) to eliminate cage to cage effects. In all studies mice were matched for sex and age.
Blinding	Where appropriate data collection was performed in a blind manner.

Reporting for specific materials, systems and methods

We require information from authors about some types of materials, experimental systems and methods used in many studies. Here, indicate whether each material, system or method listed is relevant to your study. If you are not sure if a list item applies to your research, read the appropriate section before selecting a response.

Materials & experimental systems

n/a	Involved in the study
☐	☒ Antibodies
☒	☐ Eukaryotic cell lines
☒	☐ Palaeontology
☐	☒ Animals and other organisms
☐	☒ Human research participants
☒	☐ Clinical data

Methods

n/a	Involved in the study
☒	☐ ChIP-seq
☐	☒ Flow cytometry
☒	☐ MRI-based neuroimaging

Antibodies

Antibodies used	Anti mouse APRIL antibodies (clones Apry-1-1 and 108), anti-CD16/32 antibody (clone 93; eBiosciences), anti-B220 PercP-Cy5.5 (clone RA3-6B2; eBiosciences), anti-CD23 FITC (clone B3B4; eBiosciences), anti-CD43 PE (clone S7; BD Biosciences), anti-IgM APC (clone II/41; eBiosciences), anti-CD21 biotinylated (clone 7E9; Biolegend), anti-CD11b APC (clone M1/70; eBiosciences), anti-CD5 (clone 53-7.3; eBiosciences), CD11b-APC (clone M1/70; eBiosciences), anti-Ly6C-FITC (clone HK1.4; Biolegend), anti-Ly6G-PE (clone 1A8; Biolegend), anti-flag M2 antibody (Sigma), biotinylated rat anti-mouse IgG1 (cloneA85-1; BD Biosciences), anti-mouse IgM (Sigma; M8644) or anti-mouse IgG1 (Biolegend; RMG1-1) or anti-mouse IgG2b (BD Biosciences; R9-91) or anti-mouse IgG2c (STAR135) or anti-mouse IgG3 (BD Biosciences; R2-38) or anti-mouse IgA (BD Biosciences; C10-3), anti-mouse IgM antibody conjugated to alkaline phosphatase (Sigma; A9688), biotinylated anti-mouse IgG1 (BD Biosciences; A85-1), biotinylated anti-mouse IgG2b (BD Biosciences; R12-3), anti-mouse IgG2c (JIR 115-065-208), anti-mouse IgG3 (BD

Biosciences; R40-82), anti-mouse IgA (BD Biosciences; C10-1), anti-mIgG2a-biot (rat; clone R19-15; BD), anti-flag antibody (Biolegend; clone L5), mouse anti-APRIL biotinylated antibody (clone 2C8), anti-HSPG2 (clone: A7L6; Merck Millipore), anti-CD31 (clone: EPR3094; Abcam), goat anti-rat AF488 (Life Technologies), goat anti-rabbit AF647 (Life Technologies), goat anti-mouse AF555 (Life Technologies), MB47 antibody (provided by Dr. Witztum's lab UCSD), Anti-hAPRIL antibodies Mahya-1 (mouse IgG1, AG-20B-0078PF-C100) and 110 (mouse IgG1) were provided by Adipogen. Aprily1, Aprily2, Aprily3, Aprily5, Aprily6, Aprily8, Aprily9 and Aprily10 (mouse IgG1) were custom-made by NanoTools (Teningen, Germany), mouse anti-APRIL biotinylated antibody clone 2C8, rabbit anti-ApoB antibody (Abcam; ab20737)

Validation

The validation of the commercially available antibodies used for flow cytometry and confocal microscopy were performed by antibody suppliers per quality assurance literature provided by each supplier. Extensive validation data for the antibodies that were developed by us are either included in previous publications (which are cited in the manuscript) or are included in the manuscript.

Animals and other organisms

Policy information about studies involving animals; ARRIVE guidelines recommended for reporting animal research

Laboratory animals	Ldlr-/-, Apoe-/- and Bcma-/- and Apoe-/- Hspg2d3/d3 mice were on C57BL/6J background. Female and male mice were included in the studies at the age of 8 weeks or more.
Wild animals	This study did not involve wild animals
Field-collected samples	This study did not involve samples collected from the field
Ethics oversight	All experimental studies were approved by the Animal Ethics Committee of the Medical University of Vienna (Austria) 66.009/0281-/WFV/3b/2014, 66.009/0223-WF/II/3b/2014 and 66.009/0398-V/3b/2019 or have been regulated under the Animals (Scientific Procedures) Act 1986 Amendment Regulations 2012 following ethical review by the University of Cambridge Animal Welfare and Ethical Review Body (PPL PA4BDF775).

Note that full information on the approval of the study protocol must also be provided in the manuscript.

Human research participants

Policy information about studies involving human research participants

Population characteristics	Patients from the ICARAS (Inflammation and Carotid Artery-Risk for Atherosclerosis Study) clinical study described in Schillinger, M., et al. Inflammation and Carotid Artery--Risk for Atherosclerosis Study (ICARAS). Circulation 111, 2203-2209 (2005). Patients from the LURIC study, including exclusion and inclusion criteria are described in Winkelmann, B.R., et al. Rationale and design of the LURIC study--a resource for functional genomics, pharmacogenomics and long-term prognosis of cardiovascular disease. Pharmacogenomics 2, S1-73 (2001). Patients from the FAST-MI study are described in Puymirat, E. et al Acute Myocardial Infarction: Changes in Patient Characteristics, Management, and 6-Month Outcomes Over a Period of 20 Years in the FAST-MI Program (French Registry of Acute ST-Elevation or Non-ST-Elevation Myocardial Infarction) 1995 to 2015. Circulation 10.1161/CIRCULATIONAHA.117.030798, (2017).
Recruitment	ICARAS: In this single-center study, 1268 consecutive patients who underwent duplex ultrasound investigations of the extracranial carotid arteries were prospectively enrolled between March 2002 and March 2003. A total of 1268 patients were enrolled in the study. Of these, 203 patients (16%) were lost to clinical follow-up and for 280 patients (22%) no serum sample for the measurement of APRIL levels was available, leaving 785 patients for the final analysis. The 483 patients who had to be excluded from analysis did not differ significantly from the subjects who were included with respect to baseline and demographic parameters (age, sex, frequency of risk factors for atherosclerosis, and cardiovascular comorbidities. LURIC: Patients from the LURIC study, including exclusion and inclusion criteria are described in Winkelmann, B.R., et al. Rationale and design of the LURIC study--a resource for functional genomics, pharmacogenomics and long-term prognosis of cardiovascular disease. Pharmacogenomics 2, S1-73 (2001). The exclusion and inclusion criteria for patients from the FAST-MI study are described in Puymirat, E. et al Acute Myocardial Infarction: Changes in Patient Characteristics, Management, and 6-Month Outcomes Over a Period of 20 Years in the FAST-MI Program (French Registry of Acute ST-Elevation or Non-ST-Elevation Myocardial Infarction) 1995 to 2015. Circulation 10.1161/CIRCULATIONAHA.117.030798, (2017).
Ethics oversight	The ICARAS study complied with the Declaration of Helsinki and was approved by the review board and the institutional ethics committee of the Medical University of Vienna. The LURIC study was approved by the institutional review board of the ethics committee of the Landesärztekammer Rheinland-Pfalz (No. 1997-203). All patients gave their written informed consent. The FAST-MI study was approved by the Committee for the Protection of Human Subjects in Biomedical Research of Saint Antoine University Hospital and the Commission Nationale Informatique et Liberté.

Note that full information on the approval of the study protocol must also be provided in the manuscript.

Flow Cytometry

Plots

Confirm that:

☒ The axis labels state the marker and fluorochrome used (e.g. CD4-FITC).

☒ The axis scales are clearly visible. Include numbers along axes only for bottom left plot of group (a 'group' is an analysis of identical markers).

☒ All plots are contour plots with outliers or pseudocolor plots.

☒ A numerical value for number of cells or percentage (with statistics) is provided.

Methodology

Sample preparation	Whole spleens were isolated and single cell suspensions were obtained using cell strainers with 100 µm diameter. Erythrocytes were lysed with erythrocyte lysis buffer. Flow cytometry analysis of splenic and peritoneal B and T cell subsets was performed using directly conjugated antibodies on mechanically obtained single cell suspensions of freshly isolated spleens and peritoneal cells. Peripheral blood from the vena cava was diluted with PBS + 2% dextran (Sigma) and incubated for at least 30 minutes at 37oC to concentrate the RBCs at the bottom of the tube. The upper clear phase was collected, and cells were stained with directly conjugated antibodies HUVECs were stained in DPBS (Sigma) supplemented with 10% FBS (Gibco) with 0.5µg/ml of either murine flag-tagged APRIL4 or amino-terminal flag-tagged bacterial alkaline phosphatase (BAP) fusion protein (Sigma) for 30 minutes at 4oC, followed by staining with 1µg/ml of anti-flag M2 antibody (Sigma) for 20 minutes at 4oC. Then cells were stained with 1µg/ml of a biotinylated rat anti-mouse IgG1 (cloneA85-1; BD Biosciences) for 20 minutes at 4oC and streptavidin-APC (eBiosciences) for 20 minutes at 4oC. HEK 293 wild-type cells were stained for 20 min on ice with 50 µl of Flag-ACRP-mAPRIL A88 (DYKDDDDKGPGQVQLH-[aa 18-111 of mACRP30]-LQ-[aa 88-232 of mAPRIL]) in FACS buffer (PBS+ 5% FCS) at 1000 ng/ml final and 5-fold dilutions, either alone or after preincubation with Apry1-1 at 25 µg/ml, or after preincubation with liquemine (DrossaPharm, Basel, Switzerland) at 10 I.U./ml final concentration. Then cells were stained with biotinylated anti-Flag M2 (1:500; Sigma F9291) followed by PE-coupled streptavidin. HEK 293 wild-type cells were stained with 5% rat serum in PBS+0.5% BSA (buffer) for 15 min on ice. After washing with buffer, cells were incubated with 1, or 3 or 6 µg/ml of Fc-human APRIL-A88 for 30 min on ice. After washing cells were incubated with human native LDL at 25 or 75 or 225 µg/ml for 30 min on ice. Then, cells were incubated with 4% PFA for 20 min at room temperature. After washing with buffer, cells were stained with the monoclonal MB47 antibody (provided by Dr. Witztum's lab UCSD) at 0.5µg/ml for 20 min on ice, followed by an anti-mIgG2a-biot (rat; clone R19-15; BD) for 15 min on ice and PE-coupled streptavidin for 15 min on ice (1:400; eBiosciences).
Instrument	FACS Calibur (BD) or FACS Accuri C6 (BD) or LSRFortessa (BD)
Software	BD CellQuest Pro, BD FACS Accuri C6 and LSRFortessa-FACS Diva (BD) softwares were used to collect flow cytometry data
Cell population abundance	not applicable
Gating strategy	FSC/SSC gating was used to identify live cells. B cell subsets were defined as: follicular/trantitional stage 2 B cells: B220+CD43-CD21+CD23+, marginal zone B cells: B220+CD43-CD21highCD23-, transitional stage 1 (T1) B cells: B220+CD43-CD21lowCD23-, newly formed (NF)B cells: B220+CD43-CD21l-CD23-, B-1 B cells: B220lowIgM+CD43+; peritoneal B-1a: B220lowCD11bintCD5+, B-1b: B220lowCD11bintCD5- and CD23+ B-2: B220highCD11b-CD5-CD23+ cells; CD4+ T cells : as CD3+CD4+CD8- and CD8+ T cells: CD3+CD8+CD4-, peripheral inflammatory monocytes as: CD11b+B220-Ly6G-Ly6Chigh, intermediate monocytes: CD11b +B220-Ly6G-Ly6Cint and resident monocytes: CD11b+B220-Ly6G-Ly6Clow.

☐ Tick this box to confirm that a figure exemplifying the gating strategy is provided in the Supplementary Information.